

University of Windsor

## Scholarship at UWindor

---

Electronic Theses and Dissertations

Theses, Dissertations, and Major Papers

---

2008

### A Reconfigurable Digital Multiplier and 4:2 Compressor Cells Design

Peng Chang  
*University of Windsor*

Follow this and additional works at: <https://scholar.uwindsor.ca/etd>

---

#### Recommended Citation

Chang, Peng, "A Reconfigurable Digital Multiplier and 4:2 Compressor Cells Design" (2008). *Electronic Theses and Dissertations*. 8127.  
<https://scholar.uwindsor.ca/etd/8127>

This online database contains the full-text of PhD dissertations and Masters' theses of University of Windsor students from 1954 forward. These documents are made available for personal study and research purposes only, in accordance with the Canadian Copyright Act and the Creative Commons license—CC BY-NC-ND (Attribution, Non-Commercial, No Derivative Works). Under this license, works must always be attributed to the copyright holder (original author), cannot be used for any commercial purposes, and may not be altered. Any other use would require the permission of the copyright holder. Students may inquire about withdrawing their dissertation and/or thesis from this database. For additional inquiries, please contact the repository administrator via email ([scholarship@uwindsor.ca](mailto:scholarship@uwindsor.ca)) or by telephone at 519-253-3000ext. 3208.

# **A Reconfigurable Digital Multiplier and 4:2 Compressor Cells Design**

by

**Peng Chang**

A Thesis

Submitted to the Faculty of Graduate Studies  
through Electrical Engineering  
in Partial Fulfillment of the Requirements for  
the Degree of Master of Applied Science at the  
University of Windsor

Windsor, Ontario, Canada

2008

© Peng Chang



Library and Archives  
Canada

Published Heritage  
Branch

395 Wellington Street  
Ottawa ON K1A 0N4  
Canada

Bibliothèque et  
Archives Canada

Direction du  
Patrimoine de l'édition

395, rue Wellington  
Ottawa ON K1A 0N4  
Canada

*Your file Votre référence*  
ISBN: 978-0-494-82099-5  
*Our file Notre référence*  
ISBN: 978-0-494-82099-5

#### NOTICE:

The author has granted a non-exclusive license allowing Library and Archives Canada to reproduce, publish, archive, preserve, conserve, communicate to the public by telecommunication or on the Internet, loan, distribute and sell theses worldwide, for commercial or non-commercial purposes, in microform, paper, electronic and/or any other formats.

The author retains copyright ownership and moral rights in this thesis. Neither the thesis nor substantial extracts from it may be printed or otherwise reproduced without the author's permission.

---

In compliance with the Canadian Privacy Act some supporting forms may have been removed from this thesis.

While these forms may be included in the document page count, their removal does not represent any loss of content from the thesis.

#### AVIS:

L'auteur a accordé une licence non exclusive permettant à la Bibliothèque et Archives Canada de reproduire, publier, archiver, sauvegarder, conserver, transmettre au public par télécommunication ou par l'Internet, prêter, distribuer et vendre des thèses partout dans le monde, à des fins commerciales ou autres, sur support microforme, papier, électronique et/ou autres formats.

L'auteur conserve la propriété du droit d'auteur et des droits moraux qui protègent cette thèse. Ni la thèse ni des extraits substantiels de celle-ci ne doivent être imprimés ou autrement reproduits sans son autorisation.

---

Conformément à la loi canadienne sur la protection de la vie privée, quelques formulaires secondaires ont été enlevés de cette thèse.

Bien que ces formulaires aient inclus dans la pagination, il n'y aura aucun contenu manquant.

■ ■ ■  
**Canada**

# **AUTHOR'S DECLARATION OF ORIGINALITY**

I hereby certify that I am the sole author of this thesis and that no part of this thesis has been published or submitted for publication.

I certify that, to the best of my knowledge, my thesis does not infringe upon anyone's copyright nor violate any proprietary rights and that any ideas, techniques, quotations, or any other material from the work of other people included in my thesis, published or otherwise, are fully acknowledged in accordance with the standard referencing practices. Furthermore, to the extent that I have included copyrighted material that surpasses the bounds of fair dealing within the meaning of the Canada Copyright Act, I certify that I have obtained a written permission from the copyright owner(s) to include such material(s) in my thesis and have included copies of such copyright clearances to my appendix.

I declare that this is a true copy of my thesis, including any final revisions, as approved by my thesis committee and the Graduate Studies office, and that this thesis has not been submitted for a higher degree to any other University or Institution.

# ABSTRACT

With the continually growing use of portable computing devices and increasingly complex software applications, there is a constant push for low power high speed circuitry to support this technology. Because of the high usage and large complex circuitry required to carry out arithmetic operations used in applications such as digital signal processing, there has been a great focus on increasing the efficiency of computer arithmetic circuitry. A key player in the realm of computer arithmetic is the digital multiplier and because of its size and power consumption, it has moved to the forefront of today's research.

A digital reconfigurable multiplier architecture will be introduced. Regulated by a 2-bit control signal, the multiplier is capable of double and single precision multiplication, as well as fault tolerant and dual throughput single precision execution.

The architecture proposed in this thesis is centered on a recursive multiplication algorithm, where a large multiplication is carried out using recursions of simpler sub-multiplier modules. Within each sub-multiplier module, instead of carry save adder arrays, 4:2 compressor rows are utilized for partial product reduction, which present greater efficiency, thus result in lower delay and power consumption of the whole multiplier.

In addition, a study of various digital logic circuit styles are initially presented, and then three different designs of 4:2 compressor in Domino Logic are presented and simulation results confirm the property of proposed design in terms of delay, power consumption and operation frequency.

***To my beloved parents.***

# ACKNOWLEDGEMENTS

There are several people who deserve my sincere thanks for their generous contributions to this thesis.

I would first like to express my sincere gratitude to my supervisor Dr. Majid Ahmadi for all of his generous support and guidance. His guidance and advice both academically and personally have had, and will continue to have, a tremendous impact on my life. He has been an excellent mentor to me. To him I am deeply indebted.

I would also like to thank the faculty at the University of Windsor, including Dr. Roberto Muscedere for the many conversations and advice offered, and my committee members, Dr. Arunita Jaekel and Dr. Mitra Mirhassani for their patience and support.

Ms. Andria Turner also deserves much thanks and recognition. Her dedication to the students is second to none. For all of her assistance and cheerful conversation I am extremely appreciative.

To Mr. Liton Ghosh, Mr. Ashkan Hosseinzadeh Namin, Mr. Neil Scott, and Mr. Anthony Karlof, Ms. Mazad Azarmehr I also offer great gratitude. Their sound technical advice has not only contributed to this thesis but their friendship made the late nights in the lab all the more bearable.

Finally, to my parents I must extend my most sincere love and gratitude. For every path I have chosen, they have always shown unending support and enthusiasm.

# Table of Contents

<b>AUTHOR'S DECLARATION OF ORIGINALITY .....</b>	<b>iii</b>
<b>ABSTRACT.....</b>	<b>iv</b>
<b>DEDICATION.....</b>	<b>v</b>
<b>ACKNOWLEDGEMENTS .....</b>	<b>vi</b>
<b>LIST OF FIGURES .....</b>	<b>x</b>
<b>LIST OF TABLES .....</b>	<b>xii</b>
<b>CHAPTER 1 INTRODUCTION .....</b>	<b>1</b>
1.1 Introduction .....	1
1.2 Thesis Highlights.....	2
1.3 Thesis Organization.....	3
<b>CHAPTER 2 DIGITAL MULTIPLICATION .....</b>	<b>4</b>
2.1 Basics of Digital Multiplication .....	4
2.2 Sequential Multiplication .....	6
2.2.1 Shift-Add Multiplication .....	6
2.2.2 High Radix Multipliers.....	7
2.3 Parallel Multipliers.....	8
2.3.1 Linear parallel Multipliers.....	9
2.3.2 Column Compression Multipliers .....	10
2.4 Partial Product Reduction Techniques .....	12
2.4.1 CSA Reduction Scheme .....	13
2.4.2 4:2 Compressor Reduction Scheme.....	16



## **CHAPTER 3 A RECONFIGURABLE MULTIPLIER ARCHITECTURE . 20**

3.1	Recursive Multiplication Algorithms.....	20
3.1.1	Background Information.....	21
3.1.2	6:2 Reduction Circuitry .....	24
3.2	A Reconfigurable Multiplier Architecture .....	27
3.2.1	Double Precision Mode .....	30
3.2.2	Single Precision Mode.....	31
3.2.3	Dual Single Precision Mode.....	32
3.2.4	Single Precision Fault-tolerant Mode .....	33
3.3	Modeling and Simulation.....	34
3.3.1	HDL Model.....	34
3.3.2	Implementation and Layout.....	35
3.3.3	Simulation Results.....	36

## **CHAPTER 4 CIRCUIT LEVEL DESIGNS OF 4:2 COMPRESSORS ..... 38**

4.1	High Order Counters and Compressors .....	38
4.1.1	Counters.....	38
4.1.2	Compressors .....	39
4.2	4:2 Compressors.....	41
4.2.1	Structure of 4:2 Compressors .....	41
4.2.2	Logical Level Decompositions of 4:2 Compressors.....	42
4.3	Circuit Level Designs of 4:2 Compressors .....	45
4.3.1	Static CMOS.....	47
4.3.2	Transmission Gate Logic.....	48
4.3.3	Pass Transistor Logic.....	49
4.3.4	Dynamic Logic .....	50

4.4	Domino Logic .....	51
4.5	Circuit Level Optimizations of Domino Logic Gates .....	58
4.5.1	Multiple-output Domino Logic .....	58
4.5.2	Split Domino Logic .....	62
4.6	Simulation Result .....	64
4.6.1	Simulation Result for Logical Level Decompositions of 4:2 Compressors .....	65
4.6.2	Simulation Result for Circuit Level Designs of Full adder and 4:2 Compressor .....	67
<b>CHAPTER 5 CONCLUSIONS.....</b>		<b>72</b>
5.1	Summary of Contributions .....	72
5.1.1	Architectural Contributions .....	72
5.1.2	Transistor Level Contributions .....	73
5.2	Conclusions .....	73
<b>REFERENCES.....</b>		<b>74</b>
<b>VITA AUCTORIS.....</b>		<b>77</b>

# LIST OF FIGURES

Figure 1 4x4 bit multiplication leading to an 8-bit product .....	5
Figure 2 A simple dot diagram of 16-bit partial product array .....	6
Figure 3 Shift-add multiplier implementation .....	7
Figure 4 Shift-add implementation of a basic radix-4 multiplier .....	8
Figure 5 One sided CSA tree forming an Array Multiplier .....	10
Figure 6 Schematic representation of the column compression multiplier process.....	11
Figure 7 Carry Save Adder (CSA) Array .....	12
Figure 8 12x12 Wallace Tree.....	14
Figure 9 12x12 Dadda Tree .....	15
Figure 10 Definition of a 4:2 Compressor Row.....	17
Figure 11 Compressor layout for a 16×16-bit multiplication .....	19
Figure 12 Dot diagram of a single level recursive <i>n-bit</i> multiplication.....	23
Figure 13 A schematic of a single level recursive multiplier .....	23
Figure 14 A standard 6:2 reduction microcell composed of 3 stages of full adders.....	24
Figure 15 6:2 Microcells capable of receiving a variety of input bits .....	25
Figure 16 A modified version of 6:2 reduction block.....	27
Figure 17 Outline of Reconfigurable Multiplier .....	29
Figure 18 Double precision mode.....	30
Figure 19 Single precision mode .....	31
Figure 20 Dual single precision mode .....	32
Figure 21 Single precision – fault tolerant mode.....	33
Figure 22 Layout view of designed 64-bit reconfigurable multiplier .....	36
Figure 23 General Counter Representation.....	39

Figure 24 General Compressor Representation .....	40
Figure 25 Symbol of 4:2 compressor.....	42
Figure 26 Architecture level representation of 4:2 compressor.....	43
Figure 27 Primitive decomposition of 4:2 compressor at gate level (Com_and) .....	43
Figure 28 Two alternative decompositions of 4:2 compressor at gate level.....	45
Figure 29 Static CMOS logic cell depicting the NFET and PFET networks .....	47
Figure 30 Transmission Gate.....	48
Figure 31 Pass-transistor implementation of an AND gate .....	49
Figure 32 Primitive representation of dynamic Logic block .....	51
Figure 33 Domino Logic.....	52
Figure 34 Leakage issues in dynamic circuits .....	54
Figure 35 Static keeper compensate for the charge leakage .....	55
Figure 36 Charge sharing in dynamic circuits .....	56
Figure 37 4:2 compressor in Domino Logic (Com_D).....	57
Figure 38 Multiple-output domino logic.....	59
Figure 39 Full adder in multiple-output domino logic (FA_new_D) .....	60
Figure 40 Full adder in multiple-output domino logic (FA_D).....	61
Figure 41 4:2 compressor in multiple-output domino logic (Com_new_D) .....	61
Figure 42 n-input split domino (SD) OR gate .....	62
Figure 43 Full adder in split domino logic (FA_new_SD).....	63
Figure 44 4:2 compressor in split domino logic (Com_new_SD) .....	64

# LIST OF TABLES

Table 1 Max column height per stage of a 3:2 scheme (carry save adder array) .....	16
Table 2 Max column height per stage of a 4:2 scheme (4:2 compressor array) .....	16
Table 3 Modes of Operation of the Reconfigurable Multiplier .....	29
Table 4 Simulation Results for Reconfigurable Multipliers .....	37
Table 5 Simulation Results for logical decompositions of 4:2 Compressors .....	66
Table 6 Comparison of different logical decompositions of 4:2 Compressors .....	66
Table 7 Simulation Result for full adders .....	68
Table 8 Comparison of Simulation Result.....	68
Table 9 Simulation Result for 4:2 compressors.....	69
Table 10 Comparison of Simulation Result.....	70

# CHAPTER 1

## INTRODUCTION

### 1.1 Introduction

Prior to 1935, a computer was known as a person who performed arithmetic calculations or “one who computes” Computer was actually a job title during this period of time. The modern machine definition is based on von Neumann’s concepts [1]: “a device that accepts input, process data, stores data, and produces output” While technology has come a long way in the many years since von Neumann’s work, the basic formula for the components of a computing system have remained the same.

Von Neumann and his associates state that “a general purpose computing machine should contain certain main organs relating to arithmetic, memory-storage, control and connection with the human operator” [1]. The arithmetic organ is known today as the *arithmetic logic unit (ALU)*; it is required to be capable of adding, subtracting, multiplying, and dividing. This thesis deals specifically with the multiplication function of this arithmetic organ.

Multiplication is the key arithmetic operation which is widely used in many microprocessors and digital signal processing applications. Microprocessors use multipliers within their arithmetic logic units, and digital signal processing systems require multipliers to implement DSP algorithms such as convolution and filtering. Since the multiplier lies directly within the critical path in most systems, the demand for high-

speed multiplier is continuously increasing [1]. However, with the fast growing of portable computing devices, the power consumption of the multiplier has become equally important. All this has resulted in the pursuit of high speed low power multiplier design techniques.

## **1.2 Thesis Highlights**

This thesis will present a general investigation of digital multiplication, and will highlight novel reconfigurable multiplier architecture. The proposed design utilizes the reconfigurable architecture and an optimized 4:2 compressor rows distribution methodology for partial product reduction presented by Mokrian et al [6]. The principle advantage of this scheme lies in its multi-mode reconfiguration ability and high efficient partial product reduction.

The proposed scheme combines many desirable design characteristics, such as low power dissipation, high throughput capabilities, and fault tolerance. Moreover, a 64-bit reconfigurable multiplier, with potential applications in Digital Signal Processor (DSP) devices, has been implemented using the TSMC 0.18  $\mu\text{m}$  technology. This design has been contrasted against a standard high performance architecture of equivalent size, and has demonstrated promising results, which will be presented in chapter 3.

In addition, other investigations into circuit level implementations of 4:2 compressor will be addressed. In particular, various designs of 4:2 compressor in Domino Logic are presented and simulation results confirm the property of proposed designs in terms of delay, power consumption and operation frequency.

## 1.3 Thesis Organization

The thesis will begin with a general overview of the concept of digital multiplication, and various multiplication algorithms in chapter 2. Moreover, this chapter will present the fundamentals of partial product reduction.

Chapter 3 will focus on the introduction of the reconfigurable multiplier architecture, beginning with the outline of the recursive multiplication algorithm, followed by implementation and simulation results.

Chapter 4 will initially introduce the 4:2 compressor in terms of basic functionality. This will be followed by an in-depth analysis of logic styles used in the construction of 4:2 compressors. This analysis will include proposed 4:2 compressor designs in Domino Logic. This chapter will conclude with the simulation and comparison among these designed circuitries in terms of delay, power consumption and operation frequency. This thesis will conclude with a summary of contributions and conclusions in chapter 5.



# CHAPTER 2

## DIGITAL MULTIPLICATION

### 2.1 Basics of Digital Multiplication

Prior to exploring the various multiplication algorithms, and the applications of each, it is imperative to present the essence of digital multiplication, and the standard nomenclature. Just as in the paper and pencil methodology of carrying a multiplication of two values, digital multiplication entails a sequence of additions carried out on partial products. The means by which this partial product array is summed to yield the final product is the key distinguishing factor amongst multiplication schemes.

In general, the partial product array for an  $M \times N$  bit multiplication is formed by the bitwise logical AND of the *multiplicand*  $A$  and *multiplier*  $X$ , where:

$$X = [x_m, x_{m-1}, x_{m-2} \dots x_2, x_1, x_0]$$

$$A = [a_n, a_{n-1}, a_{n-2} \dots a_2, a_1, a_0]$$

The summation of the partial products will yield an  $(n+m)$ -bit product,  $P$ , where:

$$P = [s_{n+m}, s_{n+m-1}, s_{n+m-2} \dots s_2, s_1, s_0]$$

The partial product array will have  $(n \times m)$  bits, arranged in  $m$  rows of  $n$ -bit values. The array is in essence composed of a sequence of rows that are either shifted versions of the

**multiplcand**,  $A$ , or zeros, according to the bits of the **multiplier**,  $X$ . The multiplication of two 4-bit values is illustrated in Figure 1.

		$a_3$	$a_2$	$a_1$	$a_0$		
	$X$	$x_3$	$x_2$	$x_1$	$x_0$		
		$x_0a_3$	$x_0a_2$	$x_0a_1$	$x_0a_0$		
		$x_1a_3$	$x_1a_2$	$x_1a_1$	$x_1a_0$		
		$x_2a_3$	$x_2a_2$	$x_2a_1$	$x_2a_0$		
		$x_3a_3$	$x_3a_2$	$x_3a_1$	$x_3a_0$		
$s_7$	$s_6$	$s_5$	$s_4$	$s_3$	$s_2$	$s_1$	$s_0$

**Figure 1 4x4 bit multiplication leading to an 8-bit product**

To better visualize the partial product reduction process, the concept of dot diagrams shall be introduced [1, 2]. A dot diagram is a visual representation of the bits in an algorithm, where in this particular application the dots represent individual partial product bits. The nature of the dot diagram is to depict the bits using the relative position of individual bits, and the manner in which they are manipulated, irrespective of the actual value of each bit.

Figure 2 shows the partial product array for a 16x16-bit multiplication [1]. The partial products are shifted to account for the differing arithmetic weight of the bits in the multiplier, where dots of the same arithmetic weight are aligned vertically. The final product, represented by the double length row of dots at the bottom, is obtained via the summation of the dots in each column.

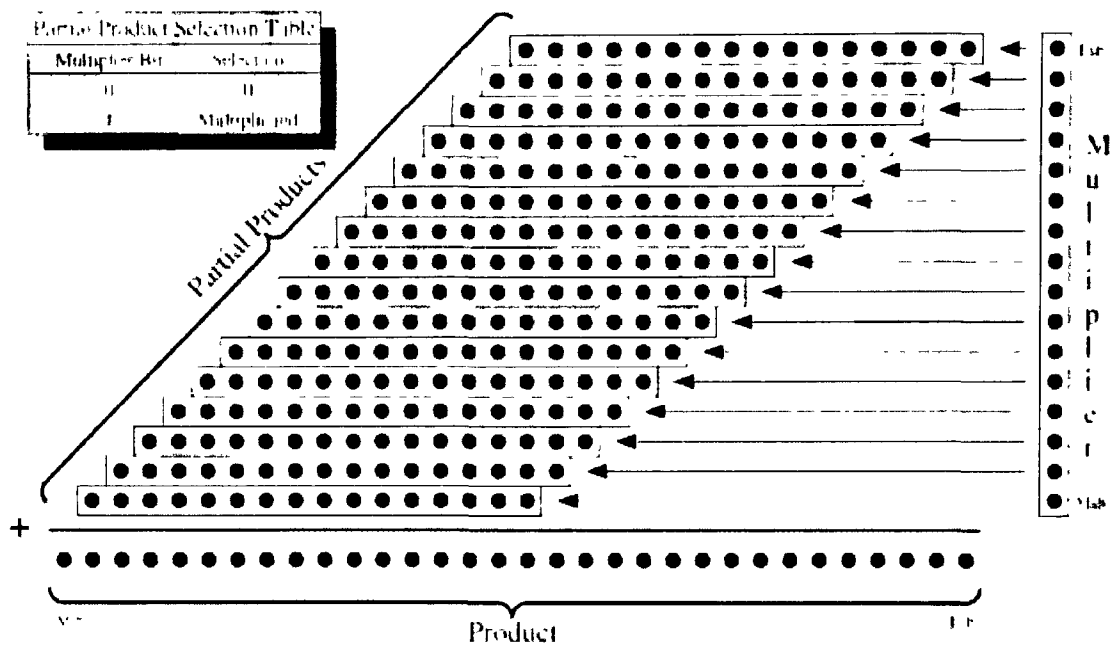
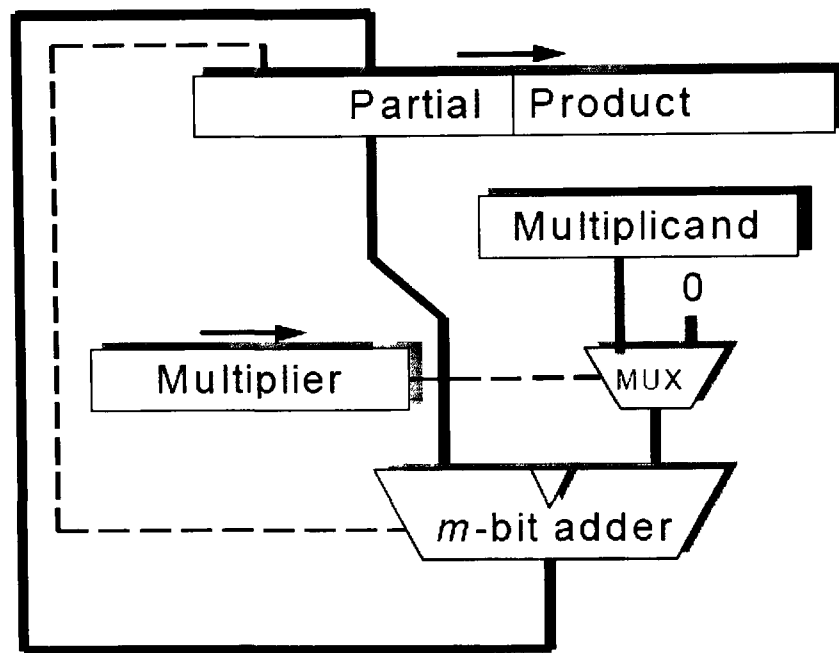


Figure 2 A simple dot diagram of 16-bit partial product array

## 2.2 Sequential Multiplication

### 2.2.1 Shift-Add Multiplication

In its most basic form, digital multiplication may be carried out through a sequence of shifts and additions of the *multiplier* to the *partial product* register, governed by the individual bits of the *multiplier* (Figure 3). This primitive form of multiplication, known as shift-add or iterative multiplication, although very simple in implementation, is very slow. The number of iterations, or cycles of addition, that are required grows linearly with the size of the *multiplier*, with each cycle having a delay of the required fast adder.



**Figure 3 Shift-add multiplier implementation**

### 2.2.2 High Radix Multipliers

A variation of this rudimentary form of digital multiplication is the high-radix multiplication algorithm. Though fundamentally identical to the shift and add algorithms, these multipliers accept more than one bit of the *multiplier* on each clock cycle. This process reduces the number of clock cycles required to carry out a multiplication, at the added expense of the requirement for the immediate availability of fixed multiples of the *multiplicand*.

Figure 4 provides an outline for a radix-4 multiplication scheme, where each clock cycle now utilizes two bits of the *multiplier*, effectively doubling the throughput over a conventional radix-2 binary multiplier [3]. Note that in this scheme, a separate register is required to store the previously multiplied value of 3A. The higher the radix of the multiplier, the more stored values that will be required. Through the use of higher radix multipliers (radix-8, radix-16, etc.), the greater the achievable computation speeds;

however, this comes at the expense of increased overhead in terms of shift circuitry, and storage registers for all of the required multiples of the multiplicand.

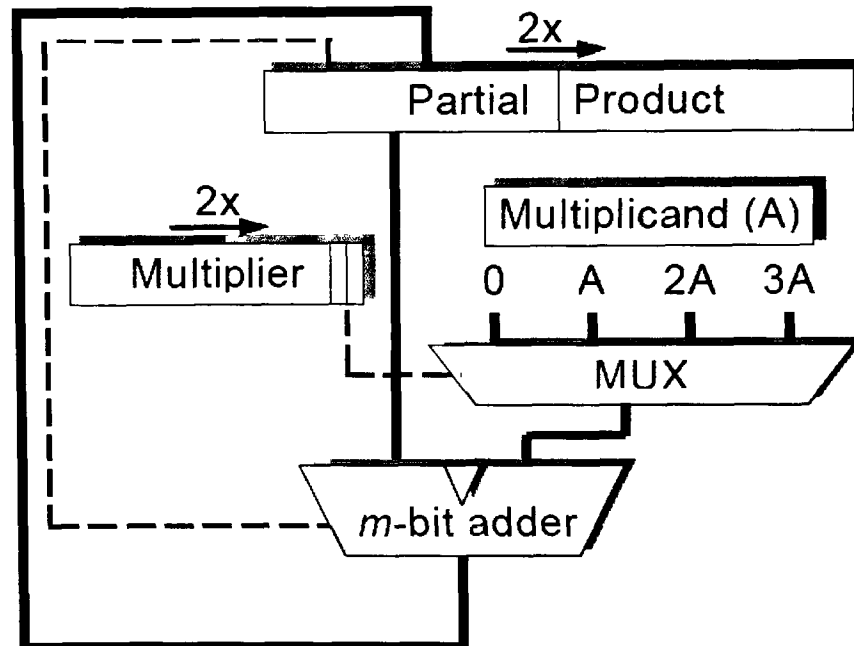


**Figure 4 Shift-add implementation of a basic radix-4 multiplier**

## 2.3 Parallel Multipliers

Serial multipliers, and the concept of shift and add algorithms, are a class of primitive multiplication schemes that take advantage of simple implementation techniques. Such methods are employed where hardware overhead is an issue, or if there is a lack of a dedicated hardware multiplier. Modern high performance machines call for more sophisticated algorithms, in order to limit the computation latency.

Parallel multipliers in general may be classified into two distinct categories: linear parallel multipliers, and column compression multipliers. As opposed to the serial multiplier, parallel multipliers generate all of the partial products simultaneously. In

addition, parallel multipliers limit the latency associated with carry propagation to one final fast adder.

### **2.3.1 Linear parallel Multipliers**

Linear parallel multipliers often referred to as array multipliers; obtain their name from the linear relationship between their latency and operand size. The array multiplier may be regarded as a one sided CSA tree, where the reduction process occurs in ordered stages.

The highly regular layout of the array structure is depicted in 5-bit multiplier in Figure 5. The systematic arrangement of the cells makes this design ideal for automated layout techniques, where the bits of the two operands are broadcast across the arrangement of full adder cells. In this scheme, the outputs of the adders trickle horizontally and vertically accordingly until the perimeter of the structure where the product bits are attained. The drawback of this scheme is that the partial products are introduced and reduced one row at a time, not in parallel as in column compression multipliers. This leads to higher gate count, and slower performance.

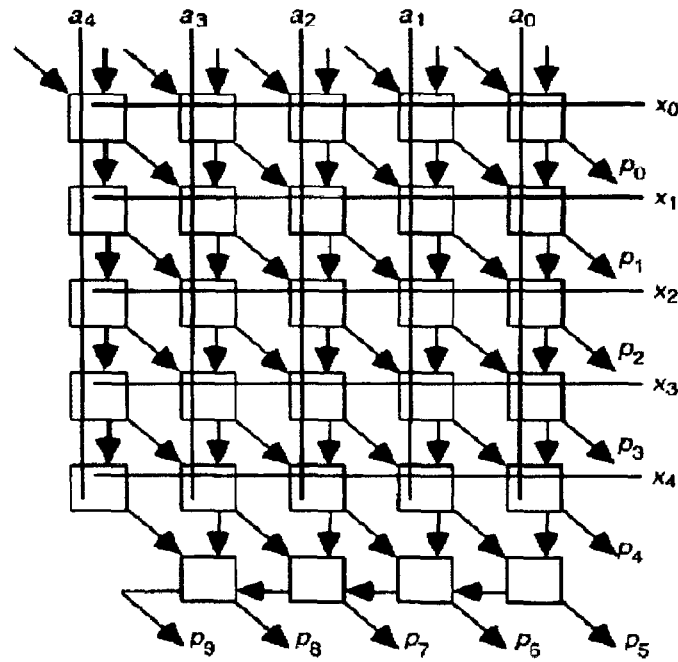


**Figure 5 One sided CSA tree forming an Array Multiplier**

### 2.3.2 Column Compression Multipliers

The foundation for the modern column compression multiplier was set forth in the 1960's by the works of C.S. Wallace, Luigi Dadda, and the Russian mathematician Yu Ofman [4, 5, 6]. The tree multiplier offers the potential for a logarithmic increase in delay relative to operand size. Once formed, the bits in the partial product array are passed onto a reduction network, which performs a column-wise compression of the bits, forming two final partial products. A final stage fast adder is used to sum the two resulting partial products. A schematic representation of this process is depicted in Figure 6 [1].

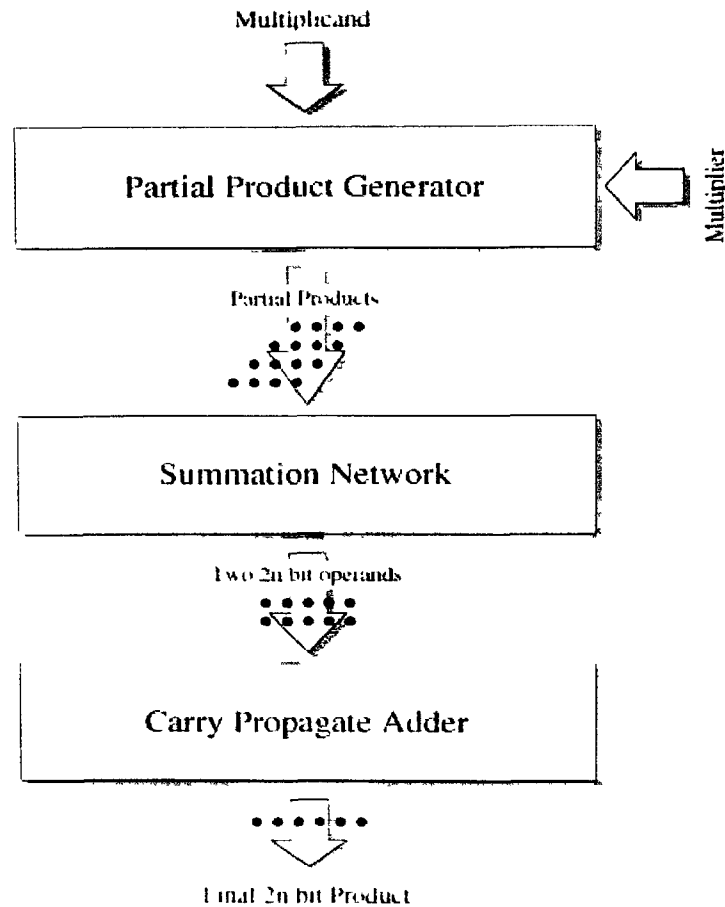


**Figure 6 Schematic representation of the column compression multiplier process**

The methodology initially proposed by Wallace [4], makes use of Carry-Save Adder (CSA) arrays in order to carry out the column-wise compression of the partial product bits. The CSA is the most commonly used form of multi-operand adder, and it is simply composed of a series of non-interlinked Full-Adder blocks, as shown in Figure 7. Through the use of such compression techniques, the carry propagation is postponed until the final stage, where the resulting partial products are summed.



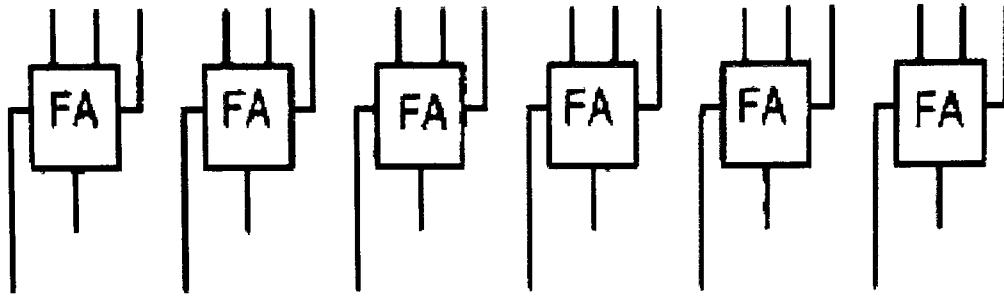


**Figure 7 Carry Save Adder (CSA) Array**

Luigi Dadda proposed a systematic methodology for laying out the CSA reduction tree such that the minimum number of counters is used [5]. In his investigation, Dadda deduced that by determining the minimum number of required stages required for the partial product reduction process, 3:2 or even higher order counters may be placed in such a manner as to minimize the hardware requirement. Since its inception, Dadda's minimum circuitry paradigm has been critically analyzed and confirmed [2, 7], and further explored for high order and heterogeneous counter arrays [8].

## **2.4 Partial Product Reduction Techniques**

The predominant distinguishing factor amongst column compression multiplier schemes lies in the manner in which the column wise compression of the partial products occurs. A desired aspect of system behavior, such as speed, area, layout or power, may be optimized by the proper selection of a particular approach. In the subsequent sections, methodologies that concentrate on these major design criteria will be presented.

## 2.4.1 CSA Reduction Scheme

Parallel tree multiplier architecture using carry save adder (CSA) arrays has formed the fundamental framework for the design of high-speed parallel multipliers over the past four decades. In this section, the dissimilarities between the Wallace and Dadda techniques will be presented.

In 1964, Wallace [4] introduced a new column compression architecture for fast multiplication as an alternative to array multiplication. His scheme involves three basic steps:

1. Generate all partial products at the same time using AND gate array.
2. Reduce all partial products to two numbers using (3, 2) and (2, 2) counters.
3. Sum the two final numbers using some form of fast addition such as a carry-look-ahead adder (CLA).

Wallace's method involves grouping all rows in each stage of partial product reduction into groups of three during each reduction stage. All columns in each group containing 3 bits are reduced using (3, 2) counters, also known as full-adders, and all columns containing 2 bits are reduced using (2, 2) counters, also known as half-adders. All rows that are not part of a three row set are then transferred to the next stage without modification. It is apparent that the Wallace method for column compression reduces the most digits at the earliest possible time. Figure 8 shows the reduction process for a 12x12-bit multiplication.

In contrast to the linear growth of delay as word length increases in array multipliers, when using this column compression architecture, delays proportional to the logarithm of the operand word size may be achieved. Therefore, column compression parallel multipliers are faster than array multipliers.

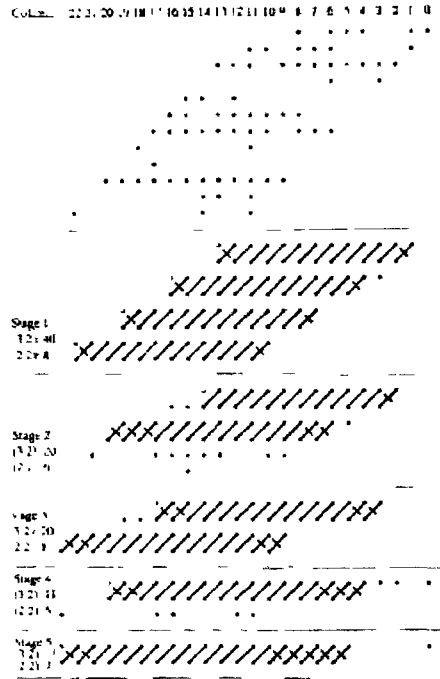


**Figure 8 12x12 Wallace Tree**

Shortly after Wallace presented his method for partial product reduction using CSA column compression, Dadda [5] was able to improve on his method by utilizing a unique placement strategy for the reduction stage counters. Like Wallace's method, Dadda uses the same three step process described earlier but unlike Wallace's method of reducing as many bits as possible at the earliest possible time, Dadda's method involves strategically reducing only some columns of each stage. This is done in order to reduce the overall number of (3, 2) counters required for the entire process. The process for reduction in a Dadda multiplier is developed using the following method, and the reduction process for a 12x12 –bit multiplication is shown in Figure 9.

1. Find the smallest  $j$  such that at least one column of the original partial product matrix has more than  $d_j$  bits where  $d_j$  is the height of the  $j^{th}$  stage from the end

$$d_{j-1} = \lfloor 1.5 \cdot d_j \rfloor$$

$$d_1 = 2$$

2. In the  $j^{th}$  stage from the end, employ (3, 2) and (2, 2) counters to obtain a reduced matrix with no more than  $d_j$  bits in any column.
3. Let  $j = j-1$  and repeat step 2 until a matrix with only two rows is generated.

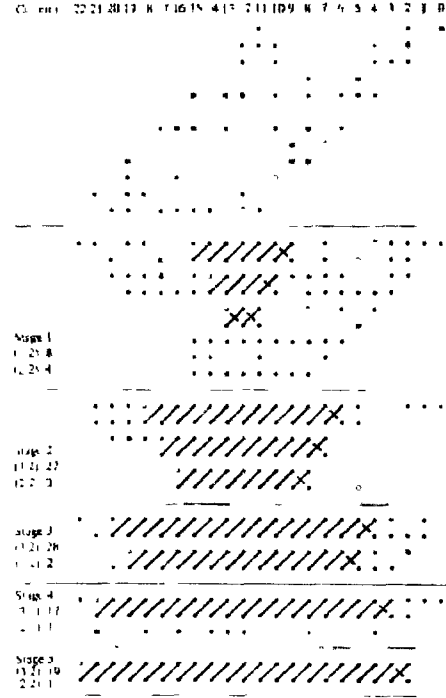


**Figure 9 12x12 Dadda Tree**

These two schemes were more recently analyzed by Bickerstaff et al. [2] further confirming that the Dadda tree does in fact utilize fewer adders during the reduction process, while the Wallace tree tends to insert adders at the earliest opportunity. Although slightly more irregular, the Dadda scheme presents a more efficient design.

### 2.4.2 4:2 Compressor Reduction Scheme

Since their inception by Weinberger [9], 4:2 compressor have become the topic of considerable research in the arithmetic community. The 4:2 compressor has transformed the standard frame of mind of counter based partial product reduction schemes by introducing the notion of horizontal data paths within stages of reduction.

The 4:2 compressor row is formed by a series of 4:2 compressors cascaded together, It is used to perform 4:2 column-wise compression of the partial product. The following tables display the relationship between column height and the number of required stages. In Table 2, the 4:2 compressor arrays, which perform 4:2 column-wise compression, are displayed, and the carry save adder arrays are also presented in Table 1.

***Table 1 Max column height per stage of a 3:2 scheme (carry save adder array)***

$h$	0	1	2	3	4	5	6	7	8	9	10
$n(h)$	2	3	4	6	9	13	19	28	42	63	94

***Table 2 Max column height per stage of a 4:2 scheme (4:2 compressor array)***

$h$	0	1	2	3	4	5	6	7
$n(h)$	3	4	8	16	32	64	128	256

As shown in tables, the 4:2 compressor based partial product reduction scheme is more efficient. For example, to reduce a column height which is 64, by using carry save adder, 9

reduction stages are required, however, by using 4:2 compressor rows, only 5 stages are needed to finish the partial product reduction.

An arbitrary distribution of 4:2 compressor rows, though effective, may not be entirely efficient. Until recently, Mokrian et al. [10] proposed a reduction scheme for using 4:2 compressors in partial product reduction. He introduced a layout scheme to minimize the number of compressor cells required in a complete reduction procedure, which follows the same idea as Dadda 3:2 counter scheme [5]. This layout scheme defines a compressor row as depicted in Figure 10. These rows begin with a half-adder or in the rightmost least significant position followed by a chain of 4:2 compressors and ending with a full-adder in the leftmost or most significant position.

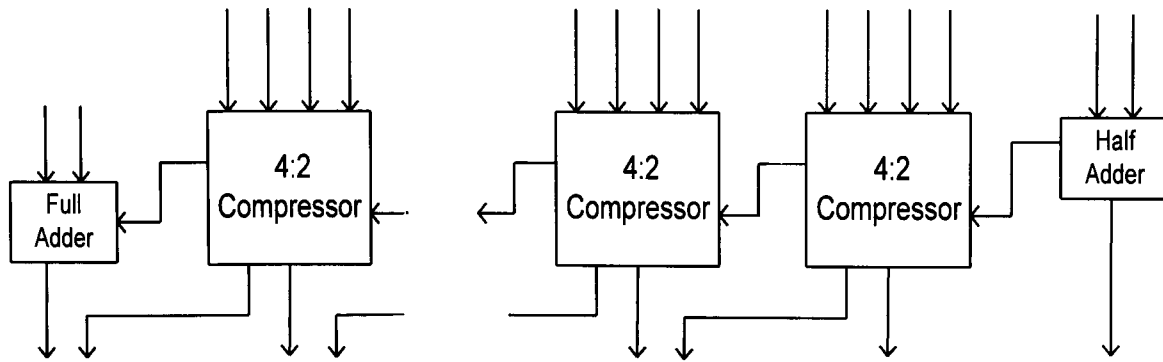


**Figure 10 Definition of a 4:2 Compressor Row**

An iterative procedure defined for implementation of this scheme is as follows [11]:

**Step (1)** Determine the number of compressor rows ( $N_R$ ) required for the given stage according to the equation:

$$N_R = \left\lceil \frac{(n(h) - 2^{\lceil \log_2 n(h) - 1 \rceil})}{2} \right\rceil \quad (1)$$

where the expression,  $2^{\lceil \log_2 n(h) - 1 \rceil}$ , refers to the maximum column height for the next stage.

**Step (2)**  $N_R$  rows of 4:2 compressors, as outlined in Figure 10, are placed in the partial product reduction tree. The first row will begin at column  $J_{1F}$  and end at column  $J_{1L}$ .

$$J_{1F} = 2^{\lceil \log_2 n(h)-1 \rceil} \quad (2)$$

$$J_{1L} = 2k - 1 - 2^{\lceil \log_2 n(h)-1 \rceil} \quad (3)$$

Every subsequent row will begin at column:

$$J_{iF} = 2^{\lceil \log_2 n(h)-1 \rceil} + 2i \quad (4)$$

$$J_{iF} = J_{(i-1)F} + 2i \quad (5)$$

and end at column:

$$J_{iL} = (2k - 1 - 2^{\lceil \log_2 n(h)-1 \rceil}) - 2i \quad (6)$$

$$J_{iL} = J_{(i-1)L} - 2i \quad (7)$$

where  $i$  is the row number within each stage up to  $N_R$ .

**Step (3)** Repeat steps (1) and (2) until only two rows remain within the partial product matrix, at which point a final fast adder will be used. In this thesis, the above scheme will be used to implement 4:2 compressors in a reconfigurable multiplier architecture.

This process is better explained through the aid of a graphic example. Figure 11 provides an example of the minimized 4:2 compressor cell distribution for 16×16-bit multiplication [10]. The symmetric layout of the compressor rows, in addition to the general configuration of each row (beginning with a half-adder and ending with a full-adder) is now evident.

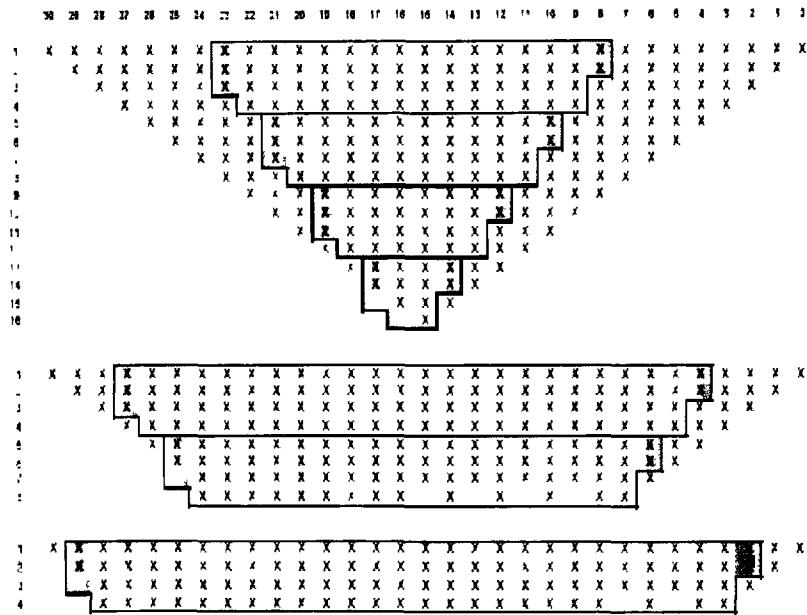


**Figure 11 Compressor layout for a 16×16-bit multiplication**



# CHAPTER 3

## A RECONFIGURABLE MULTIPLIER ARCHITECTURE

### 3.1 Recursive Multiplication Algorithms

The notion of carrying out multiplication by breaking up the operands into smaller sections has been in existence for several decades. Such schemes offer several advantages over performing standard multiplication. By breaking a large multiplication into recursions of smaller multiplications, the regularity of the design is increased, since smaller multipliers are inherently less complex. In addition, fewer, shorter interconnects are required to carry out the multiplication, with a limited number of global lines used to collect the final outputs of each recursion [10].

The name “Recursive Multiplier” may at first appear misleading, since in the implementation of this algorithm, there are no recursions, or repeated iterations of the same procedure. The process is simply broken down into smaller sub-processes which are carried out in parallel. However, for the sake of consistency with the authors [12] the same nomenclature is adopted.

### 3.1.1 Background Information

One of the pioneering schemes for "divide and conquer", or recursive, multiplication was proposed by Karatsuba and Ofman in 1962, and translated from Russian into English in 1963 [6]. The Karatsuba-Ofman Algorithm (KOA) gets the multiplication of two long integers by executing multiplications and additions on their divided parts. The KOA as described by Christof Paar [13] allows for a low complexity multiplier in Galois Fields. A field is an algebraic structure in which the operations of addition, subtraction, multiplication, and division (except by zero) can be performed while satisfying the standard rules. A Galois field is a finite field with  $p^n$  elements generated as the set of polynomials with coefficients in a modulo of an irreducible polynomial of degree  $n$ , and  $p$  is a prime integer [14].

The discussion of fields and the Karatsuba-Ofman Algorithm are beyond the scope of this thesis; however the fundamental principles of the KOA are used in the recursive algorithm presented by Danysh and Swartzlander [12]. Mathematically, the recursive algorithm may be proven by first considering two unsigned  $n$ -bit operands, the *multiplier*  $A$  and *multiplicand*  $B$ :

$$A = \sum_{k=0}^{n-1} A_k \cdot 2^k \quad (1) \quad B = \sum_{k=0}^{n-1} B_k \cdot 2^k \quad (2)$$

By dividing each of the two operands into two  $m$ -bit values, where  $m = n/2$ , we obtain:

$$A = \sum_{k=0}^{m-1} A_k \cdot 2^k + \sum_{k=m}^{2m-1} A_k \cdot 2^k \quad (3)$$

$$B = \sum_{k=0}^{m-1} B_k \cdot 2^k + \sum_{k=m}^{2m-1} B_k \cdot 2^k \quad (4)$$

$A$  and  $B$  may now be redefined as:

$$A = A_H + A_L \quad (5)$$

$$B = B_H + B_L \quad (6)$$

The overall multiplication of A and B is given by:

$$\begin{aligned}
 P &= A \cdot B \\
 &= (A_L + A_H) \cdot (B_L + B_H) \\
 &= A_H \cdot B_H + A_H \cdot B_L + A_L \cdot B_H + A_L \cdot B_L \\
 &= P_0 + P_1 + P_2 + P_3
 \end{aligned} \tag{7}$$

Therefore, the one multiplication could be reduced to four smaller sub-multiplications, and this process may be further repeated using even smaller sub-multipliers. In order to minimize the delay caused by this recursive algorithm, the result of the sub-multipliers will be kept in carry save form, and one final fast adder will be required to yield the final product.

Each of the 4 *n-bit* intermediary products in carry save format will occupy a given series of bit positions. By examining the results of the expanded multiplication outlined above, the following relationship for the positions may be deduced:

$$\begin{aligned}
 P_0 &\Rightarrow [0 \quad n-1] \\
 P_1 &\Rightarrow \left[ \frac{n}{2}-1 : \frac{3n}{2}-1 \right] \\
 P_2 &\Rightarrow \left[ \frac{n}{2}-1 : \frac{3n}{2}-1 \right] \\
 P_3 &\Rightarrow [n \quad 2n-1]
 \end{aligned}$$

A dot diagram representation of the multiplication is outlined in Figure 12, and a schematic representation is provided in Figure 13. It becomes apparent that there will be 3 intermediary products that will overlap from bit  $(n/2 - 1)$  to  $(3n/2 - 1)$ . Consequently, that leads to 6 bits that must be reduced to 2 to provide one final product in carry save form. A 6:2 reduction scheme has been proposed for the recursive multiplier [12, 15], which introduces at most an equivalent delay of three full adders. The reduction circuit is formed by an interconnection of variations of the reduction sub-block depicted in Figure 14.

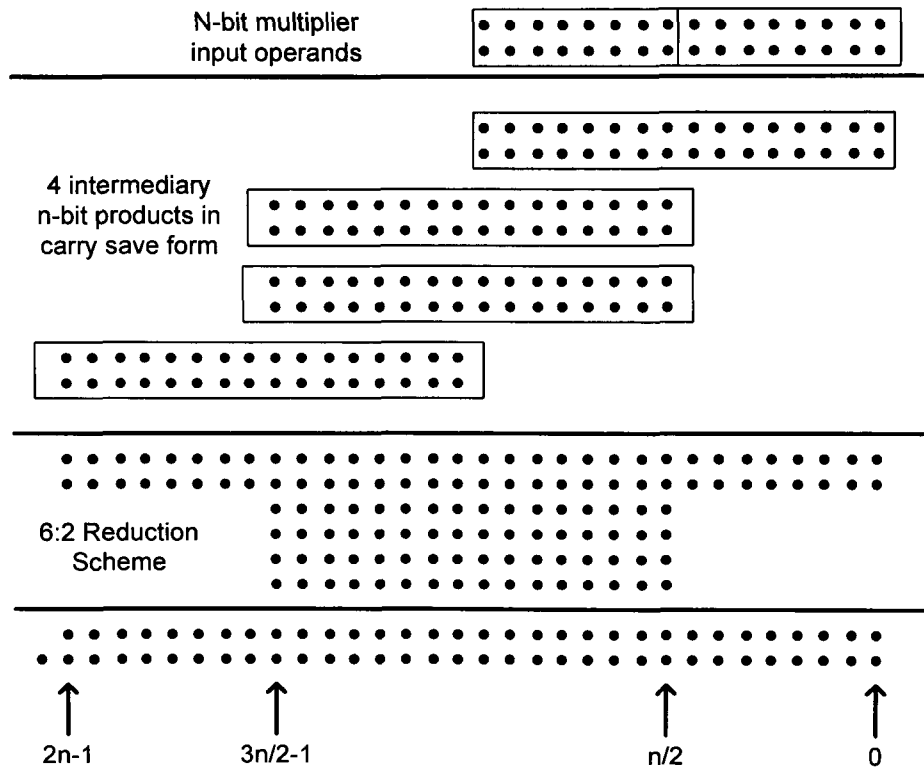


Figure 12 Dot diagram of a single level recursive  $n$ -bit multiplication

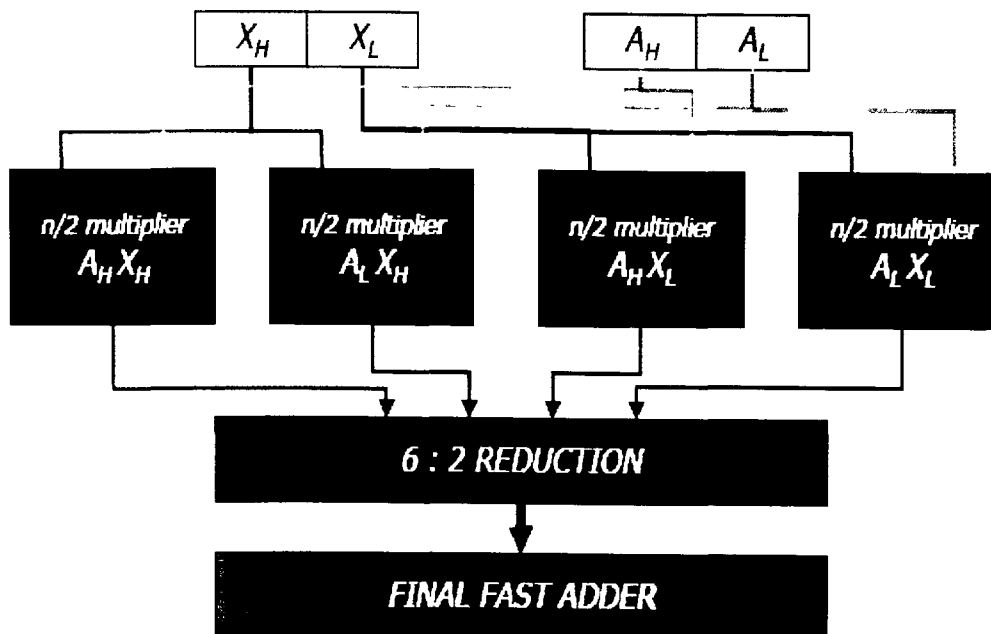
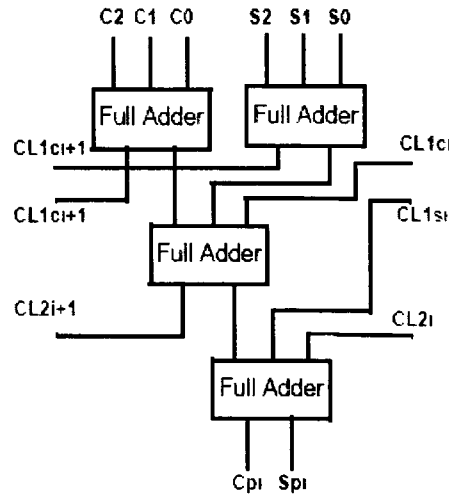


Figure 13 A schematic of a single level recursive multiplier

### 3.1.2 6:2 Reduction Circuitry

The main function of the reduction circuit is to reduce the four results generated by the intermediary multipliers down to one value, in carry save format. The 6:2 reduction block is composed of a chain of full adders generating a two bit output value, along with inter-block carry signals that propagate laterally along the reduction sub-block array. Each reduction sub-blocks will take anywhere from two to six input bits, and generate a two bit output value. In addition, there are various inter-block carry signals that propagate laterally along the reduction sub-block array. Figure 14 outlines a typical 6:2 reduction sub-block as proposed in [12]. Similar to the 4:2 compressors, the offset nature of the carry signals negates carry propagation across the reduction microcells, ensuring a maximum delay of 3 full adders for the complete process.



**Figure 14 A standard 6:2 reduction microcell composed of 3 stages of full adders**

Kim and Swartzlander [15] introduced a set of enhanced reduction sub-blocks to be used where the reduction process takes in 2, 3, 4 or 5 bit inputs. The circuits as defined in the manuscript are presented in Figure 15. It should be noted that although the circuits are not entirely efficient in their objective, they provide regularity in the reduction chain, and are capable of receiving and transmitting the carry signals without disrupting the chain.

In the architecture, two  $n$ -bit operands are bisected, resulting in 4  $n/2$ -bit sub-multiplications. The overall input to the reduction circuit arrives in a set of four  $n$ -bit values in carry save format as the output of the four intermediary multipliers. This may be more clearly defined if the dot diagram representing the overall process in Figure 12 is re-analyzed. It may be intuitively observed that the first  $n/2$  bits of the reduction circuit output may be obtained directly from the output of the multipliers. So the reduction circuitry will be required to accommodate  $3n/2$  bits of the product.

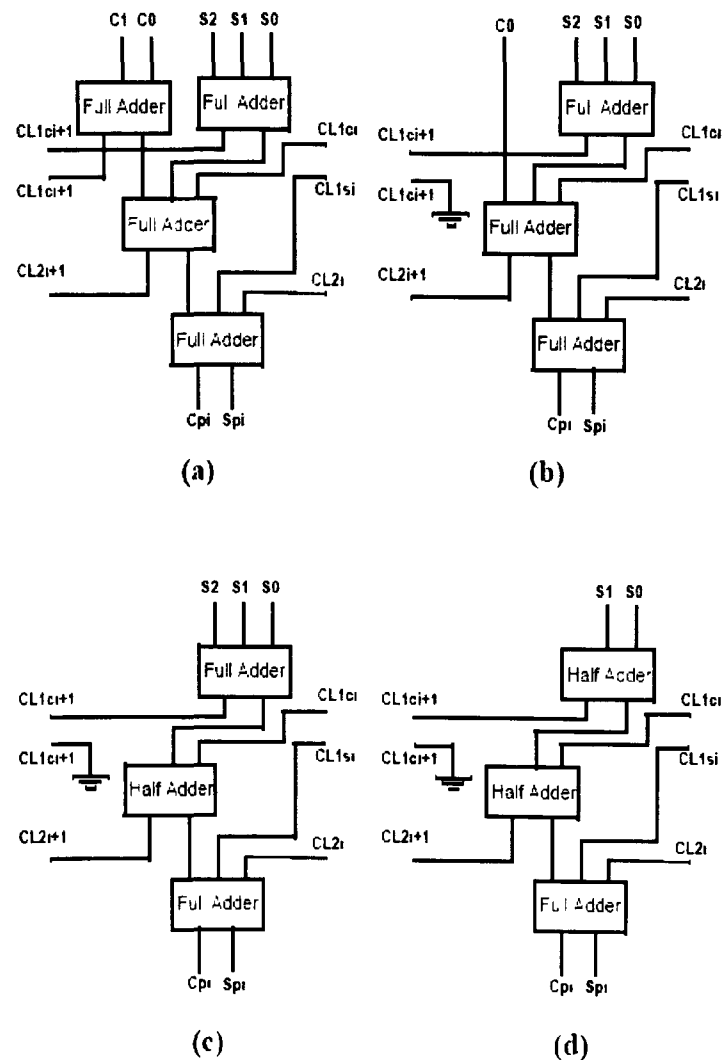


**Figure 15 6:2 Microcells capable of receiving a variety of input bits**  
**(a) 5 input (b) 4 input (c) 3 input (d) 2 input**

The reduction pattern leads to the simple expression for the allocation of the reduction sub-blocks for an  $n \times n$  bit multiplier as:

- Bits  $0$  through  $n/2-1$  are obtained directly as a result of the inputs
- Bits  $n/2$  through  $3n/2-1$  are obtained via 6-input reduction blocks
- Bits  $3n/2$  through  $2n-1$  are obtained using 2-input reduction blocks

A modified version of the presented reduction scheme is proposed by Mokrian et al. [10], and shown in Figure 16. The reduction sub-blocks having 6 inputs exist from bit position  $(n/2 - 1)$  to  $(3n/2 - 1)$ . The transition to the 2-input sub-blocks is composed of a two input reduction cell, a full adder, and a series of half adders for the remaining bits.

The need for the Half-Adder blocks, may not be obvious at first glance, however if the Carry-out of the Full-adder immediately preceding the cells is taken into consideration, then there will be three bits in position  $3n/2+1$ . Consequently, the use of the Half Adder cells will shift a carry bit laterally down the chain, allowing for the final result to have at most two bits in each position. Furthermore, it should be noted that the final carry out signal of the last Half Adder is omitted since it would be mathematically impossible to obtain a bit in the 129th position of a 64-bit multiplication. This 6:2 reduction configuration will be used for any further modification of the recursive multiplication algorithm.

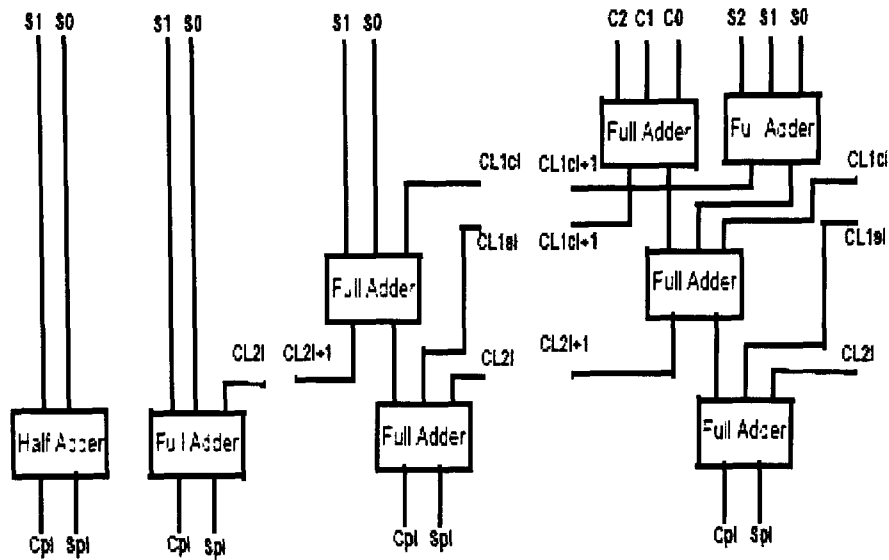


**Figure 16 A modified version of 6:2 reduction block**

### **3.2 A Reconfigurable Multiplier Architecture**

The successful design of high-speed computational systems is often predicated on the realization of advanced arithmetic circuits in digital hardware. The notions of reconfigurable architectures have been regarded as a means of adapting the hardware to achieve optimal performance under various conditions. This implies a level of intelligence built into the device for physical modification in order to meet operating requirements. The principle advantage of such systems rests in the fact that hardware realizations of computing algorithms outperform their software alternatives.

The intent of a reconfigurable architecture is to provide a means by which the performance of arithmetic hardware may be enhanced according to the desired function. For example, many modern DSP chips offer variable precision [16, 17], or fault tolerant arithmetic implemented using software [18]. The operation of these devices may be ameliorated if such functions were executed directly on hardware. Since multiplication is



considered to be the dominant computation in most digital signal processing (DSP) algorithms [19], reconfigurable multiplier architecture may prove to be a desirable augmentation to existing ALUs in the quest for maximizing performance.

Mokrian et al. [10] developed a reconfigurable multiplication architecture which envelopes the concepts of fault tolerant computing, low power design, and high throughput arithmetic into one design. The scheme utilizes a 2-bit control signal to select one of four modes of operation: double precision multiplication, single precision multiplication, dual single precision multiplication and single precision fault tolerant multiplication.

Based on Mokrian's architecture, a reconfigurable multiplier architecture is developed and shown in Fig 17, in which the 4 sub-multipliers, the reduction circuitry, the voter and the final fast adder are clearly defined. The recursive multiplier architecture with one level of recursion is used as the foundation for the reconfigurable architecture. The advantage offered by the recursive multiplication scheme is the use of smaller multipliers to implement a larger operation.

In each sub-multiplier, instead of using carry save adder array, 4:2 compressor arrays are utilized for partial product reduction, which could achieve higher partial product reduction speed.

In addition to the sub-multipliers, a series of 2:1 multiplexers are used to guide the signal flow through the device. Since all of the necessary components for each mode of operation are present in the design, there will be no reconfiguration time required. The device will be capable of switching between modes of operation in real time without the necessity to completely reconfigure the internal layout of a programmable device, as is the case with FPGA devices.

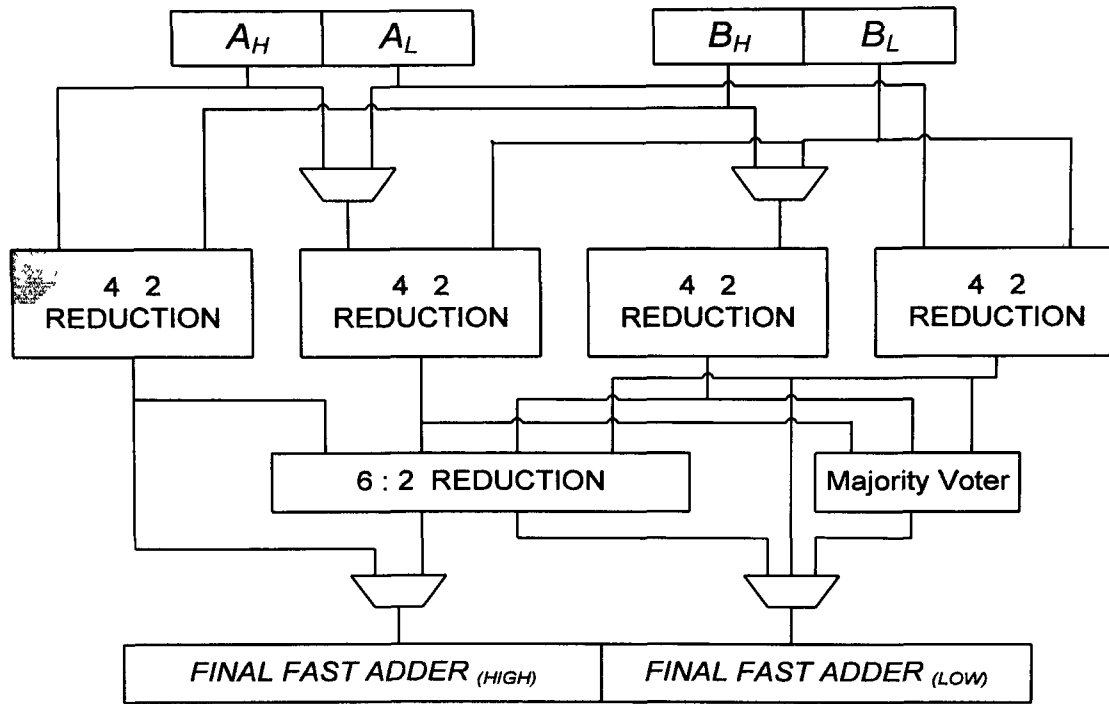


**Figure 17 Outline of Reconfigurable Multiplier**

This architecture lends itself to four modes of operation, and thus requires a 2-bit control signal for selection. The signal and the corresponding modes of operation are summarized in Table 3.

**Table 3 Modes of Operation of the Reconfigurable Multiplier**

Control Signal	Mode of Operation
00	Default – Double Precision
01	Single Precision
10	Single Precision with Fault Tolerance
11	Dual Single Precision

### 3.2.1 Double Precision Mode

The default double precision mode is simply a recursive multiplier with one level of recursion. This mode of operation reaps the benefits of the recursive multiplier architecture, while bearing no delay penalties, and minimal hardware overhead. The majority voter circuitry is disengaged through the multiplexor array (Fig 18). The reconfigurable architecture may be of any size, with the restriction that the single precision mode must be exactly one half of the double precision mode. To satisfy the IEEE floating point guidelines, a double precision multiplier having 54-bit operands is suggested, with each of the base multipliers being 27-bits wide.

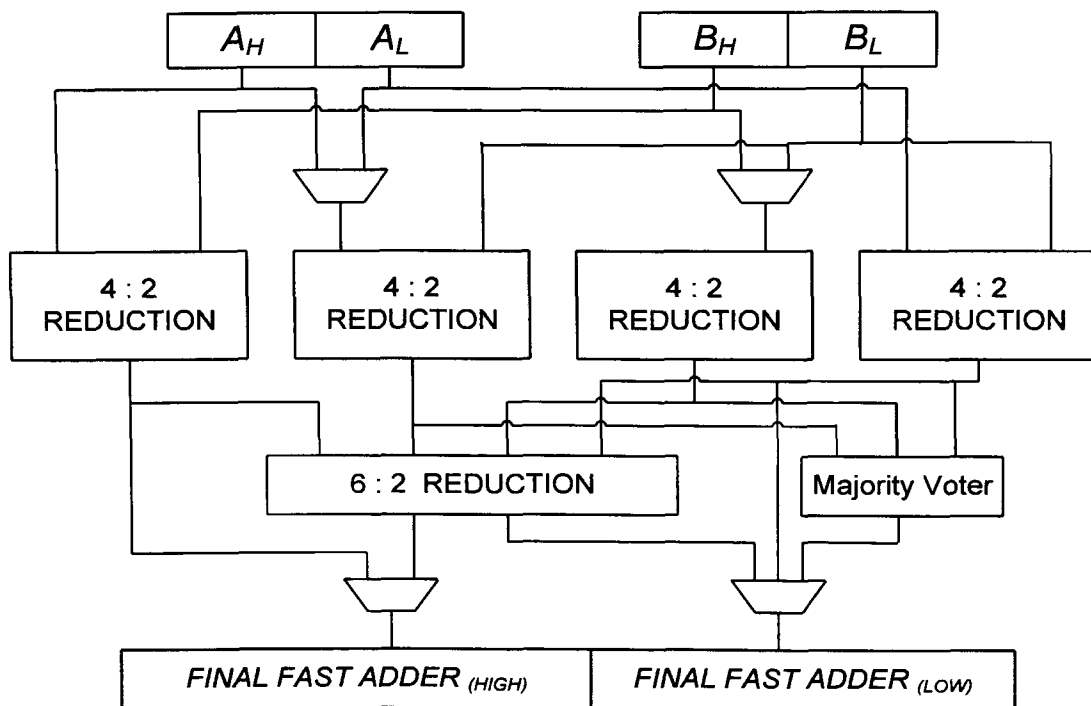


Figure 18 Double precision mode

### 3.2.2 Single Precision Mode

Single precision mode uses gating techniques to shut down three of the base multipliers, effectively cancelling over 75% of the circuit, in addition to the reduction circuitry and the majority voter (Fig 19). The final fast adder is also partitioned in the reconfigurable architecture, such that the upper portion of the adder may be shut down in order to avoid spurious transitions, which consume unnecessary power. Moreover, the overall latency now becomes that of the base multiplier, allowing faster operation in single precision mode than would be possible if the entire circuit was active.

The advantage of this scheme is that the single precision multiplication is carried out using a full single precision multiplier as opposed to shutting portions of a larger partial product reduction tree, as is proposed in other variable precision schemes [16]. In this manner, both single and double precision operations are carried out at maximum efficiency in terms of area, performance and power.

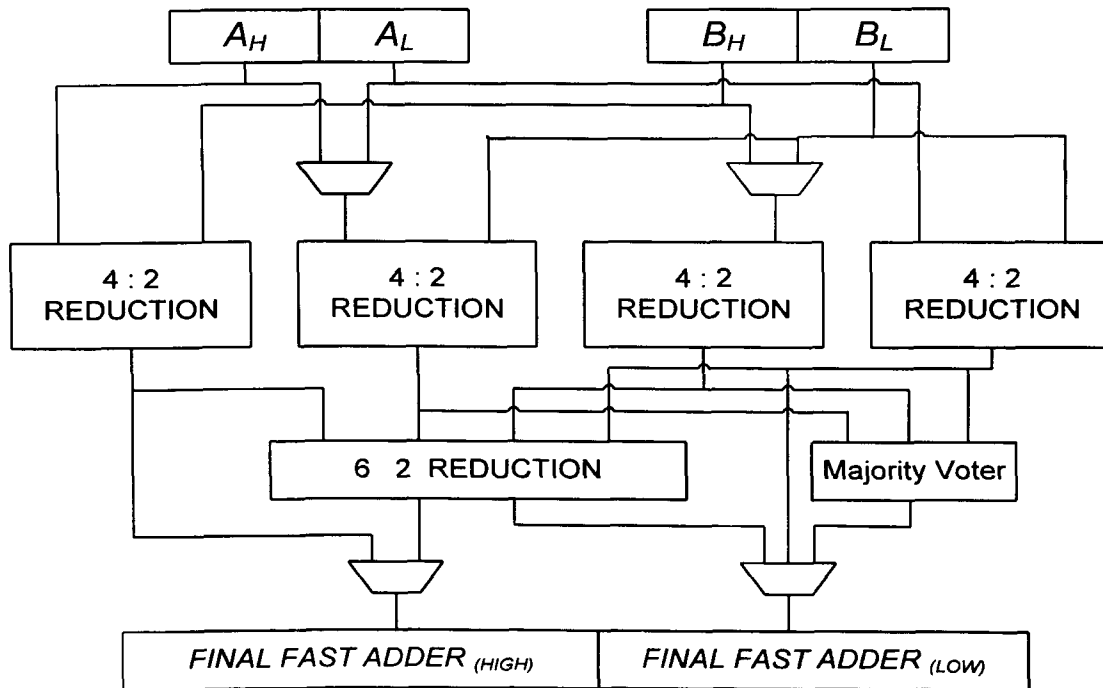


Figure 19 Single precision mode

### 3.2.3 Dual Single Precision Mode

In this operation mode, two of the base multipliers may operate in parallel on two different sets of operands, while the remaining two multipliers are inactive (Figure 20). This effectively doubles the system throughput, with a latency of a single precision multiplier. Once again, with the fast adder partitioned into two identical halves, linked via a multiplexed carry signal, two single precision fast additions may be carried out in parallel. This configuration comes at little to no delay overhead in most carry-look-ahead (CLA) and carry skip addition schemes. The gating of signals into the idle multipliers, in addition to the 6:2 reduction and majority voter circuitries allows for power savings. The idle circuits are not entirely disconnected from the power supply in order to allow for rapid and accurate engagement into any other mode of operation.

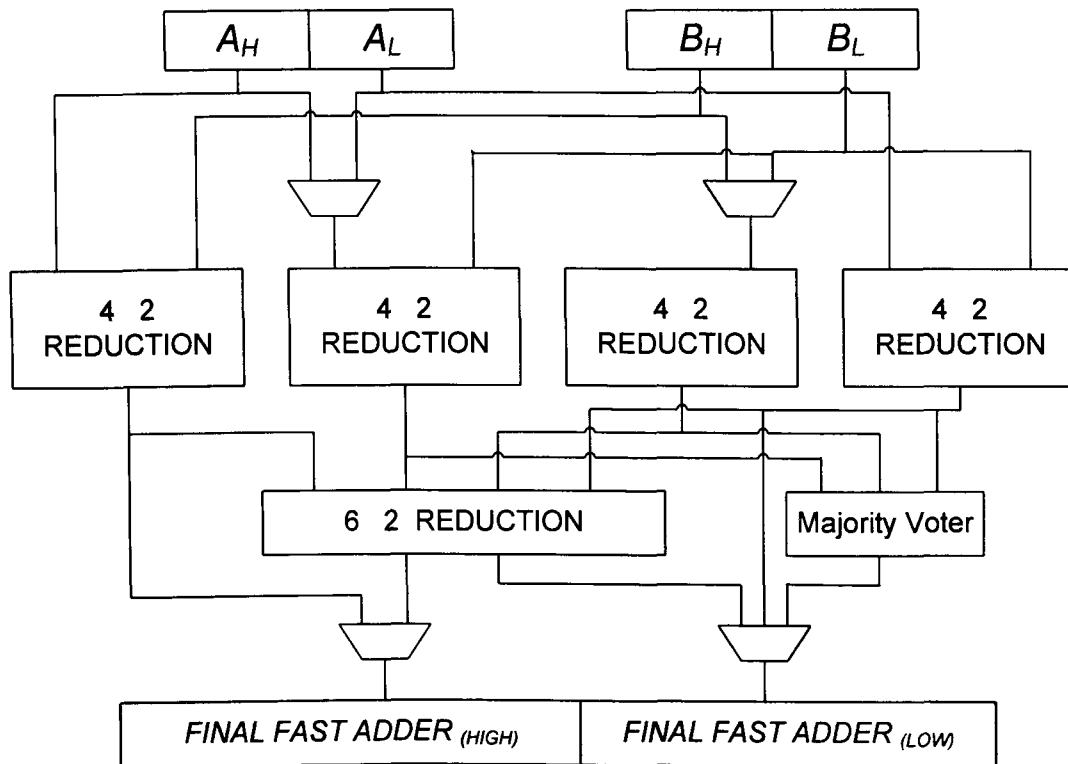
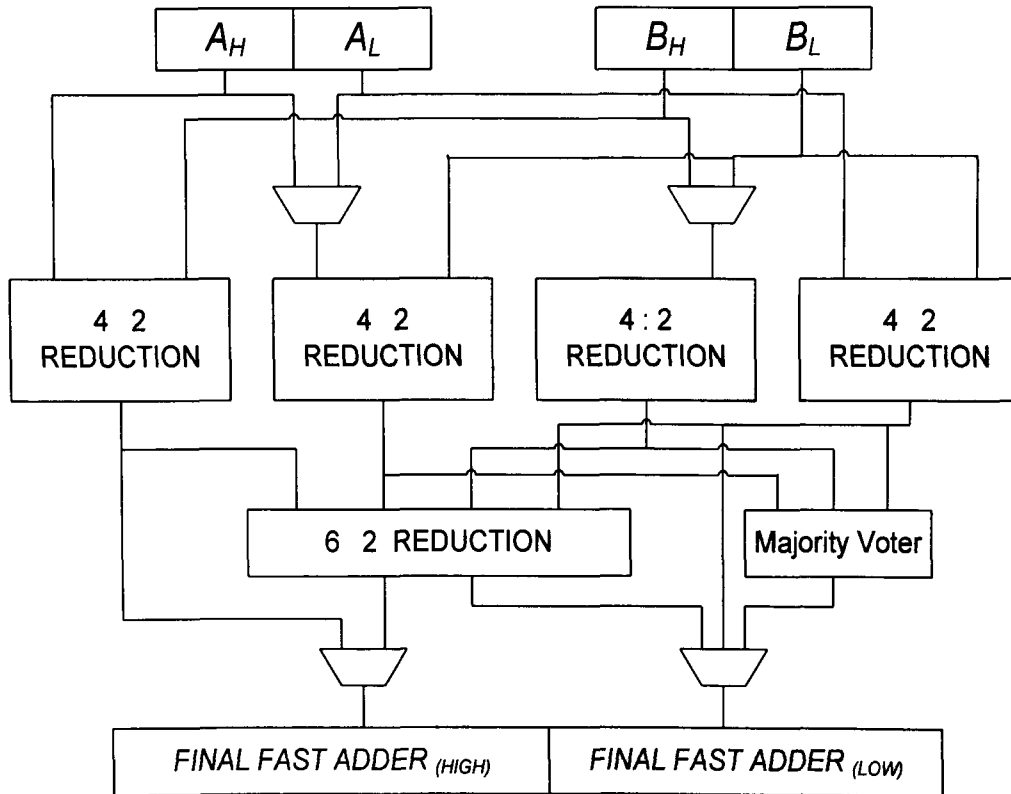


Figure 20 Dual single precision mode

### 3.2.4 Single Precision Fault-tolerant Mode

Although there are numerous methods of implementing fault tolerance in digital systems, one of the most basic methods is through majority voting between three duplicate values, which is also referred to as RETWV. Since this scheme is composed of four identical sub-multipliers, three of those may be used in conjunction with an array of 64 XOR gates and 2:1 MUX cells, to form a simple single precision fault tolerant multiplier (Figure 21).



**Figure 21 Single precision – fault tolerant mode**

With the theoretical framework for the reconfigurable multiplier architecture in place, the next section will focus on the implementation and simulation details.

### **3.3 Modeling and Simulation**

For the proper assessment of the performance characteristics of the proposed reconfigurable architecture, a valid model must be created, and compared against a benchmark model representing the state-of-the-art. For this reason, a 64-bit reconfigurable multiplier has been designed using TSMC 0.18 $\mu$ m technology. Additionally, a standard 64-bit Booth-recoded Wallace tree multiplier, similar to that employed in many of today's high performance processors, such as the Pentium IV [20], has been developed as a benchmark for comparison purposes.

#### **3.3.1 HDL Model**

Verilog describes a digital design as a set of modules, which are the basic building blocks forming the complete system. This hierarchical design methodology is a fundamental concept in Verilog digital designs. The reconfigurable multiplier design features four 32-bit sub-multipliers which are based on 4:2 compressor reduction scheme, a 48-bit 6:2 reduction block and two 64-bit carry-look-ahead adders. The overhead from the additional features are four arrays of 32 2:1 MUX cells, two arrays of 64 2:1 MUX cells, and a series of 64 XOR gates and 2:1 MUX cells for the majority voter. All of these individual modules are enveloped by the top level module which acts as a general input/output (I/O) interface for the multiplier. The top level module contains the clocked latching circuitry required for design synthesis, and does not affect the internal configuration of the multiplier itself.

The multiplier itself is partitioned into the major sections as outlined previously in Fig 17. Built in Synopsys module definitions for carry-look-ahead adders have been used to model and synthesize portions of the code, ensuring that the most efficient synthesized netlist is obtained.

The Verilog code defines the various modules and their interaction. The code in itself is over 1500 lines long, and consists of 17 different modules. A complete breakdown of the hierarchical expansion of the overall reconfigurable architecture, compiled by the Synopsys Design Vision, confirms the proper framework of the design. The standard cell components and the gate level configuration of each element may also be referenced from this file.

### **3.3.2 Implementation and Layout**

The multiplier has been implemented using the TSMC 0.18  $\mu\text{m}$  CMOS process using standard cell libraries provided by the Canadian Microelectronics Corporation. Semicustom design makes use of standard cell libraries for the fabrication of custom integrated circuits. The Cadence Design Suite, including Encounter tool, have been used for the layout placement and routing of the cells, and the layout view of designed reconfigurable multiplier is shown in Fig 22.



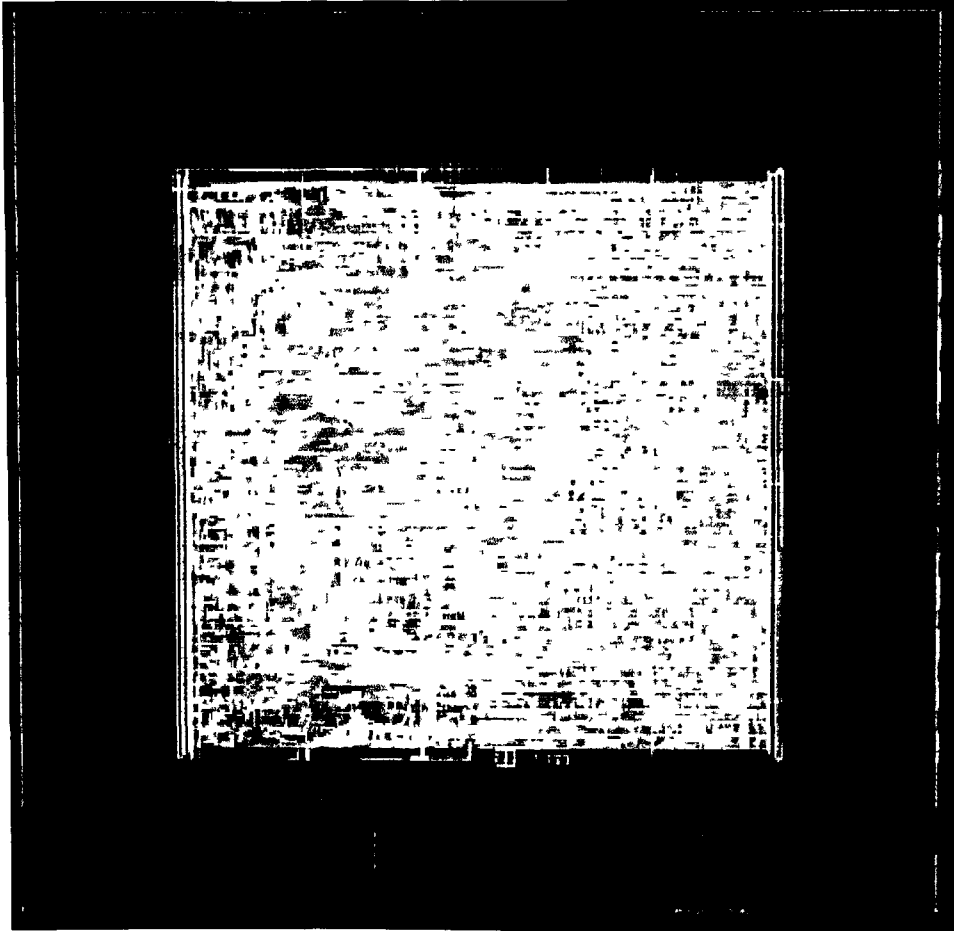


**Figure 22 Layout view of designed 64-bit reconfigurable multiplier**

### **3.3.3 Simulation Results**

As shown in the Table 4, both designed reconfigurable multiplier and benchmark multiplier are simulated in terms of functionality, power, delay and area. The simulation result verifies the proper functions of four operation modes, and highlights 25% and 19% decreases in cell internal power and total dynamic power consumption respectively. Moreover, the designed multiplier has a slightly shorter delay time, which benefits from the regularity of recursive structure. Since the designed multiplier has higher number of cells compared to benchmark multiplier, its total area and cell leakage power consumption increases 11% and 17% respectively.

**Table 4 Simulation Results for Reconfigurable Multipliers**

		<b>R.M</b>	<b>B.M M.</b>	<b>% of B.M.M</b>
<b>Area (<math>\mu\text{M}^2</math>)</b>	<i>Number of ports</i>	260	259	
	<i>Number of nets</i>	20818	4363	
	<i>Number of cells</i>	20544	3506	
	<i>Number of references</i>	63	4	
	<i>Total Area</i>	520498.9	468179.9	111.17%
<b>Power Consumption</b>	<i>Cell Internal Power (mW)</i>	162.7	214.41	75.88%
	<i>Net Switching Power (mW)</i>	146.87	164	89.55%
	<i>Total Dynamic Power (mW)</i>	309.59	378	81.9%
	<i>Cell Leakage Power (<math>\mu\text{W}</math>)</i>	26.37	22.62	116.58%
<b>Timing (nS)</b>	<i>Data Arrival Time</i>	9.84	9.9	99.39%

# CHAPTER 4

## CIRCUIT LEVEL DESIGNS OF 4:2 COMPRESSORS

### 4.1 High Order Counters and Compressors

#### 4.1.1 Counters

Although the work of Dadda has been directly linked to CSA reduction schemes, his manuscript [5] had a much broader focus, encompassing the applications of parallel counters for partial product reduction. The full adder, or carry save adder, is a particular subset of the class of parallel counters. A parallel  $(N, M)$  counter is defined as a combinational network having  $M$  outputs and inputs of equal weight, as shown in Fig 23. The  $M$  outputs are based on the number of logic 'ones' that appear at the  $N$  inputs. Any size counter may be constructed, so long as the  $M$  output bits are sufficient to represent all possible sums of the  $N$  inputs. Examples of typical counters include  $(3, 2)$ ,  $(7, 3)$ ,  $(15, 4)$ .

High order counters for partial product reduction have been explored and implemented in numerous proposals [3, 7, 8, 21, 22]. The schemes demonstrating the most promise for general multiplier architectures having arbitrary operand sizes include low order counter classes based on full adders and 4:2 compressors.

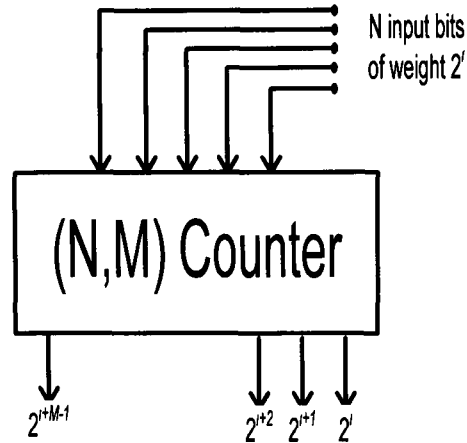


**Figure 23 General Counter Representation**

#### 4.1.2 Compressors

Similar to counter structures, digital compressors are used to reduce a given set of inputs to a vector output. The primary distinction between counter and compressor circuits is that compressors do not necessarily follow the standard pattern of  $M$  outputs drawn from  $2M$  inputs. An  $[N: M]$  compressor in essence is a variation of a counter that employs a separate path between compressor units in order to generate  $M$  final outputs using  $N > 2M$  input bits, as shown in Fig 24. Compressor configurations are generally formed using arrays of horizontally interconnected compressor units. In this manner, a horizontal carry signal may propagate laterally across the row of compressor units in order to account for the excess bits formed in the reduction process.

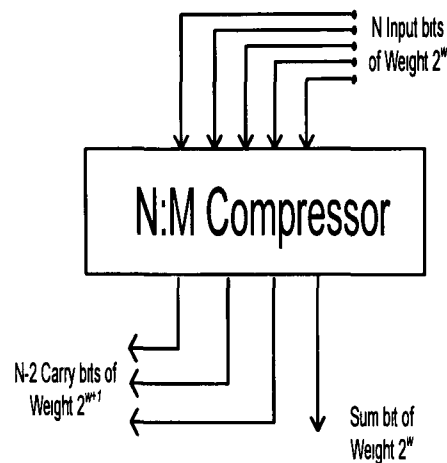


**Figure 24 General Compressor Representation**

Higher order classes of compressors may also be used using variations of large counters with horizontal interconnections; however, these circuits suffer high capacitance, large circuitry, and problematic matrix positioning as large counters. Song and DeMichelli [22] have examined the implementation of higher order compressors. Labeled as the 9:2 family of compressors, these structures are formed using 4:2 compressor and (3, 2) counters. An analysis of counters against compressors has been carried out by Mehta et al. [23]. In their research, the use of (7, 3) counters against 7:3 compressors, amongst many others, has been evaluated. Their findings illustrated no major delay advantage in the use of large compressors over large counters, except for greater interconnect complexity introduced by the inter-cell wiring of the compressors.

The most widely used style of digital compressor, which displays several promising characteristics for multiplication applications, is the 4:2 compressor. This special class of compressors requires a section of discussion on their own.

## 4.2 4:2 Compressors

Since its inception by Weinberger in 1981 [9], the concept of the 4:2 compressor has soared in popularity in many digital multiplication and multi-operand addition schemes. The application of 4:2 compressors has also been the focus of several studies promoting its use over Booth recoding schemes [24][25][26]. This section provides an in depth look at the various logical level decompositions of 4:2 compressors.

### 4.2.1 Structure of 4:2 Compressors

In general, compressors reduce N-input bits to a single sum bit of equal weight to that of the inputs but unlike counters, the remaining output bits are all of equal weight: one bit position greater than that of the inputs. Although the 4:2 compressor is not defined as a counter, since it is impossible to use 2 output bits to represent 4 binary input bits, the primitive configuration of 4:2 compressor is based on a 5:3 counter structure, which has 5 inputs and 3 outputs as shown in Figure 25. The four inputs  $X_0$ ,  $X_1$ ,  $X_2$  and  $X_3$ , and the output Sum have the same weight. The output Carry is weighted one binary bit order higher. The 4:2 compressor receives an input  $C_{IN}$  from the preceding module of one binary bit order lower in significance, and produce an output  $C_{out}$  to the next compressor module of higher significance. Different structures of 4:2 compressors exist and they all have to abide by the fundamental equation given as follows [27]:

$$X_0 + X_1 + X_2 + X_3 + C_{IN} = Sum + 2 \cdot (Carry + C_{out}) \quad (1)$$

Besides, to accelerate the carry save summation of the partial products, it is imperative that the output  $C_{out}$  be independent of the input  $C_{IN}$ .

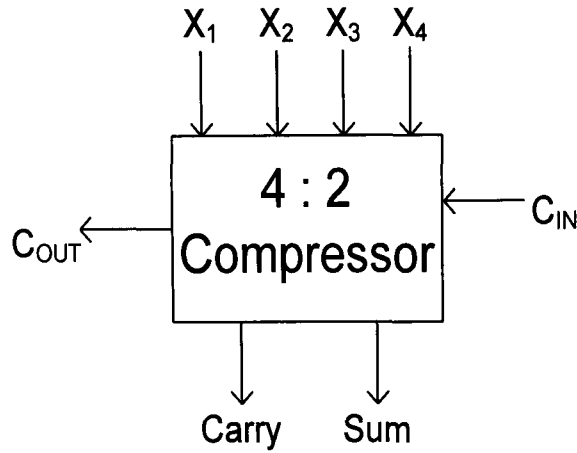


**Figure 25 Symbol of 4:2 compressor**

#### **4.2.2 Logical Level Decompositions of 4:2 Compressors**

The most primitive implementation of 4:2 compressor is that of two cascaded full adders, as shown in Figure 26 [28]. By increasing regularity, this configuration lends itself to gains at the architecture level of the multiplier. At gate level, 4:2 compressors are anatomized into XOR gates and carry generators, as shown in Figure 27. Therefore, different designs can be classified based on the critical path delay in terms of the number of primitive gates. Let  $\Delta_{\text{XOR}}$  denote the delay of an XOR gate and  $\Delta_{\text{CGEN}}$  denote the delay of a carry generator. A compressor is said to have a delay of  $(m \Delta_{\text{XOR}} + n \Delta_{\text{CGEN}})$  if its critical path consist of  $m$  XOR gates and  $n$  carry generators. Since the difference between the delays of widely used XOR gate and carry generator is trivial in an optimized design, the delay of the compressor is commonly specified as  $(m + n) \Delta$  [27]. Therefore, the straightforward implementation of a 4:2 compressor of Figure 27 has a long critical path delay of  $4\Delta$ .

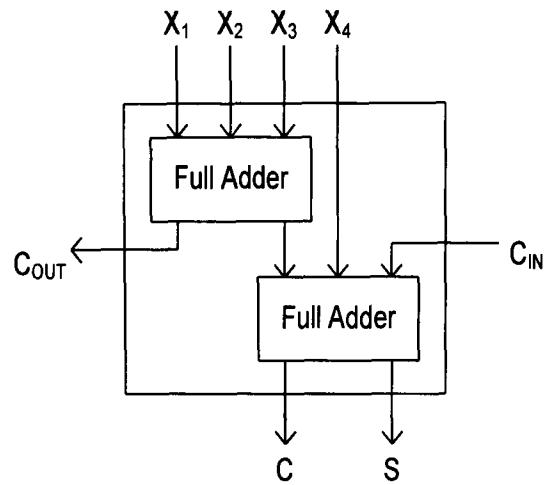


**Figure 26 Architecture level representation of 4:2 compressor**

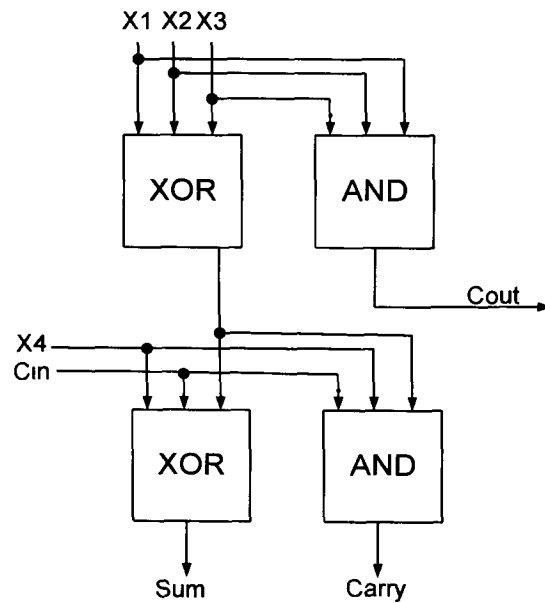


**Figure 27 Primitive decomposition of 4:2 compressor at gate level (Com\_and)**

Furthermore, alternative implementations of 4:2 compressor can be derived from its modified Boolean equations. The three outputs of the 4:2 compressor are described as follows:



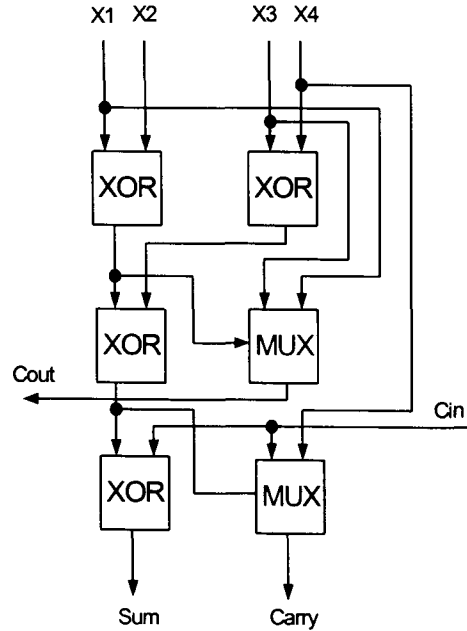
$$C_{out} = (X_0 \oplus X_1) \cdot X_2 + X_0 \quad X_1 = (X_0 \oplus X_1) \cdot X_2 + (X_0 \oplus X_1) \cdot X_0 \quad (2)$$

$$S = X_0 \oplus X_1 \oplus X_2 \quad (3)$$

$$Sum = S \oplus X_3 \oplus C_{IN} = X_0 \oplus X_1 \oplus X_2 \oplus X_3 \oplus C_{IN} \quad (4)$$

$$\begin{aligned} Carry &= (S \oplus X_3) \cdot C_{IN} + S \cdot X_3 \\ &= (X_0 \oplus X_1 \oplus X_2 \oplus X_3) \cdot C_{IN} \\ &\quad + (X_0 \oplus X_1 \oplus X_2 \oplus X_3) \cdot X_3 \end{aligned} \quad (5)$$

Figure 28 shows two logical decompositions of 4:2 compressor based on the modified Boolean equation. In Figure 28 (a), the compressor is mainly composed of six modules, four of which are XOR gates and the other two are 2:1 MUX gates. Instead of the AND gate in Figure 27, 2:1 MUX gate is used to generate two carry signals Carry and Cout. In Figure 28 (b), all three outputs Sum, Carry and Cout are generated by using 2:1 MUXs, the compressor is mainly composed of six modules, which are all XOR gates. Both implementations in Figure 28 have a critical path delay of 3  $\Delta$ , which is 1  $\Delta$  delay shorter than the primitive implementation in Figure 27. However, since a large number of inverters are required to generate complementary inputs for MUX gates, the overall circuits in Figure 28 increase their transistor count, and hence the power consumption and critical path delay, to a greater number than that of the circuit in Figure 27.



(a)

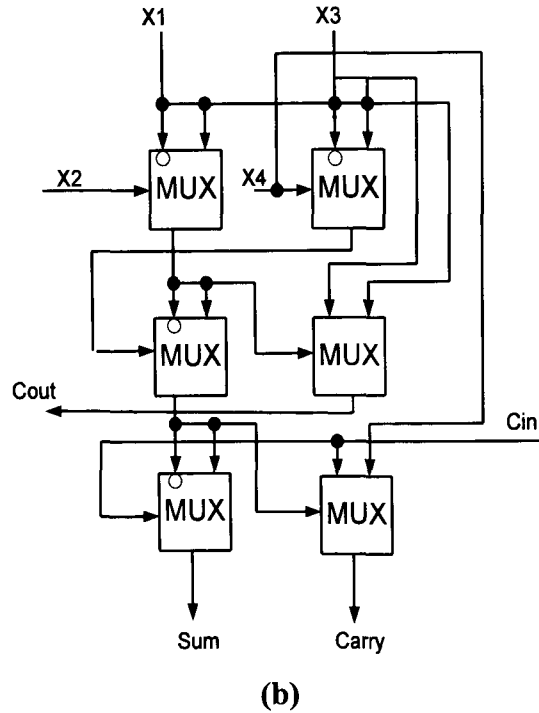


**Figure 28 Two alternative decompositions of 4:2 compressor at gate level**

**(a) Com\_mux, (b) Com\_pur\_mux**

### 4.3 Circuit Level Designs of 4:2 Compressors

Digital design encompasses a wide variety of logic implementations, which arise, for all intents and purposes, as a result of the transistor configurations composing the individual logic elements. The synthesis of the particular digital system (or sub-system) will dictate the nature of the particular logic family chosen. In a survey of logic styles, Zimmermann and Fichtner [29], outline the various characteristics of the final digital system that are dictated by the initial selection of the logic style chosen for implementation. The factors include:

- **Circuit delay:** a function of the number of inversion levels, the number of transistors in series, transistor sizes (i.e., channel widths), and intra- and inter-cell wiring capacitances.
- **Circuit size:** depends on the number of transistors and their sizes and on the wiring complexity.
- **Power dissipation:** determined by the switching activity and the node capacitances (made up of gate, diffusion, and wire capacitances), the latter of which in turn is a function of the same parameters that also control circuit size.
- **Wiring complexity:** the number of connections and their lengths in addition to the choice of single-rail or dual-rail logic.
- **Generality:** ease-of-use of logic gates in standard cell design techniques and logic synthesis.
- **Robustness:** determined by the resilience to voltage and transistor scaling as well as varying process and working conditions.
- **Compatibility:** ability to seamlessly integrate with the surrounding circuitries.

All of these characteristics may vary considerably from one logic style to another and thus make the proper choice of logic style crucial for circuit performance. Several logic styles and logic families will be presented in the following section, along with their potential vantage points and applications in arithmetic circuitry.

---

### 4.3.1 Static CMOS

Static CMOS logic, otherwise known as standard CMOS logic, is the logic style of choice for most implementations, and is most often used in the development of standard cell libraries for automated digital synthesis. The principle behind a static logic cell is that it exhibits a well-defined output once the inputs are stabilized and the switching transients have decayed away. The cell is composed of complementary NFET and PFET networks, where the input voltages control the conductance of the networks. The switching network is designed such that only one network is a closed switch for any input combination, thus determining whether  $V_{DD}$  or GND is connected to the output. Figure 29 outlines a typical static CMOS cell configuration.

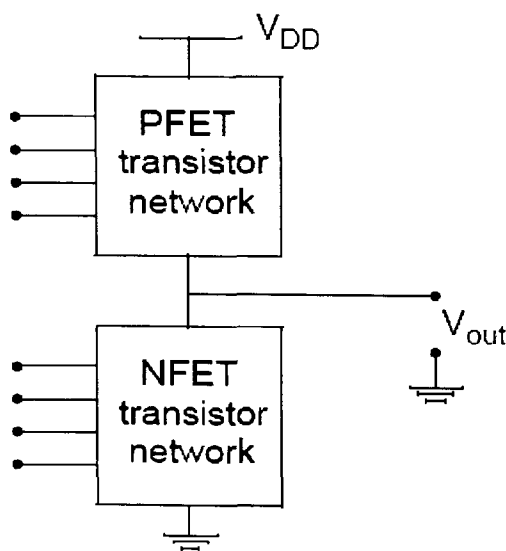


**Figure 29 Static CMOS logic cell depicting the NFET and PFET networks**

The advantage of such logic families is in the simplicity of developing a circuit that will perform a given function, however complex, while providing robust performance measures. Static logic, for the most part, demonstrates excellent noise immunity, and is less susceptible to process variation since the sizing of individual transistors does not vastly alter the circuit's functionality. One disadvantage of this type of logic is the use of

a large number of PFET devices, being both slow and large in comparison to NFETs, which increases power consumption of the circuit. Furthermore, the longest length chain within each network will determine the worst-case scenario for charge/discharge delay, forcing more complex systems to carry out potentially sluggish execution.

### 4.3.2 Transmission Gate Logic

The CMOS transmission gate (TG) is designed to act as a very efficient voltage-controlled switch, and was one of the fundamental building blocks in SSI and MSI technologies. It is formed by a parallel combination of one NFET and one PFET device, as depicted in Figure 30, set-up in such a manner as to allow a full-voltage swing output based on the control signal. The use transmission gates to form logic cells simplifies the design of many involved circuits, by allowing signals to determine the conduction path of other signals. The formation of multiplexor cells using TG logic is one straightforward application of this type of logic.

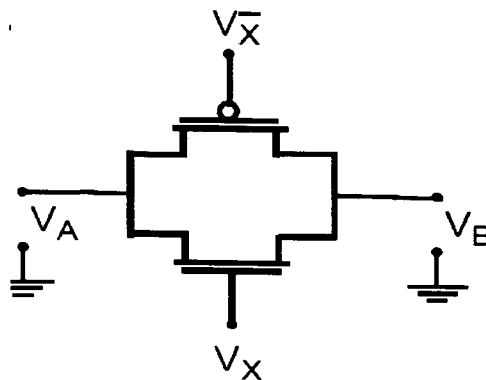


Figure 30 Transmission Gate

The downfall of TG logic lies in its requirement of a control signal and its complement, thus increasing interconnect and signal requirements. In addition, the output node does not receive voltage support since there is no pure path to either the supply voltage or to ground. For this reason the input signal must be able to drive the output capacitance, leading to potential difficulties in high fan-out applications.

### 4.3.3 Pass Transistor Logic

As an alternative to complementary CMOS, pass transistor logic attempts to reduce the number of transistors required to implement logic by allowing the primary inputs to drive source-drain terminals as well as gate terminals. Specifically, a pass transistor is a MOSFET with the input signal fed to the source and the output taken from the drain, with a control signal connected to the gate governing the output.

The promise of this approach is that fewer transistors are required to implement a given function. For example, the implementation of the AND gate in Figure 31 requires 4 transistors (including the inverter required to invert B), while a complementary CMOS implementation would require 6 transistors. The reduced number of device has the additional advantage of lower capacitance.

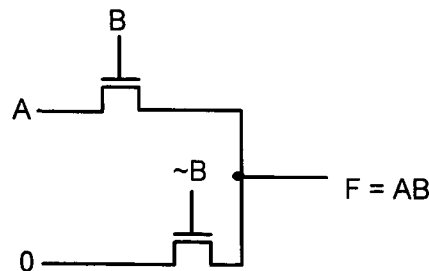


**Figure 31 Pass-transistor implementation of an AND gate**

Unfortunately, an NMOS device is effective at passing a 0, but it is poor at pulling a node to  $V_{DD}$ . When the pass transistor pulls a node high, the output only charges up to  $V_{DD} - V_{Tn}$  (threshold voltage). In fact, the situation is worsened by the fact that the device experiences body effect, because a significant source-to-body voltage is present when pulling high.

#### 4.3.4 Dynamic Logic

Standard static CMOS logic maintains a valid output voltage, so long as the inputs are well defined and continuous. Dynamic CMOS logic on the other hand makes use of capacitive nodes to store electrical charge, and so is capable of sustaining a valid output only for a short period of time. The advantages of such logic families are in their ability to quickly transfer charge, and in turn have a tremendous performance advantage over static CMOS, and are common in high speed applications. Dynamic circuits differ from static circuits in that instead of fighting the constant limits due to parasitic RC elements, capacitances are used as integral components of the circuits.

Though there are several distinct logic families that fall under the dynamic CMOS classification, there is a common underlying principle behind their operation. In general, there are two state logic styles where a clock signal controls a pair of complementary FETS managing the operation of the logic gate (Figure 32). The two stages of operation are known as the precharge and evaluate stages. During precharge, the output node is charged via the precharge PFET, this is known as “pre-conditioning” the node, while the evaluate NFET is cut off. During this phase of the clock, the output and all of the inputs are invalid. During the evaluate stage, the evaluation NFET conducts, while the precharge PFET is cut off. The inputs to the logic array are now valid, and if the logic array produces a value of '0' , there will be a conduction path for the output charge to ground, else the charge will be maintained at the output and a result of logic '1' The charge on the output node may only be held for a limited duration before being corrupted by charge leakage, and so timing is critical.

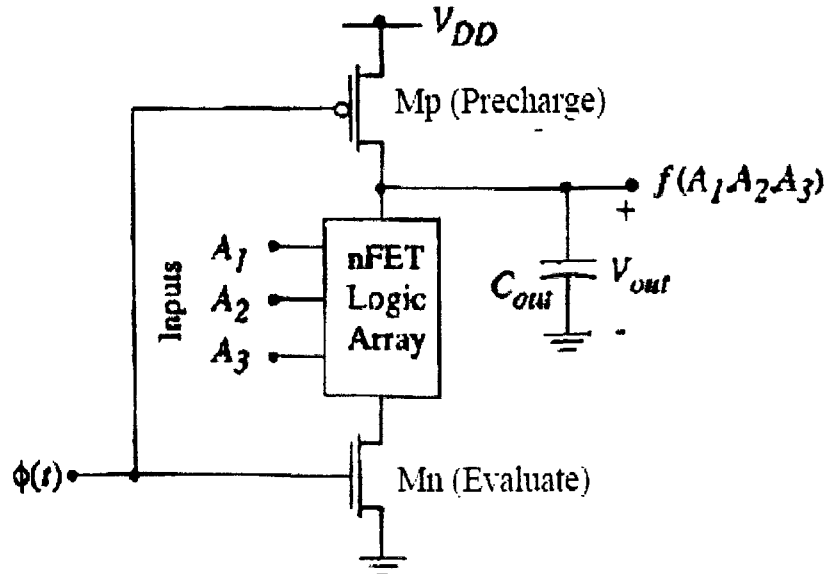


**Figure 32 Primitive representation of dynamic Logic block**

Compared to static CMOS logic, dynamic logic leads to up to 30% performance gain [30]. Therefore, speed critical paths often deploy dynamic logic to meet speed requirements. Performance gain over static logic becomes even larger as the number of inputs to the logic grows. Wide fan-in dynamic logic such as domino are often used in performance critical paths, e.g. fast look ahead adders and RAM decoders, to achieve high speeds where static CMOS fails to meet performance objectives. The following sections will be focused on domino logic and its applications in 4:2 compressors.

## 4.4 Domino Logic

A dynamic system may be formed through the simple cascading of the individual cells. This leads to the formation of a variation of the precharge-evaluate logic known as Domino Logic. The cascading of NFET logic array for the standard precharge-evaluate logic poses a potential glitch problem, which is overcome in domino logic through the inversion of the output signal between cascaded cells.



A domino logic module consists of an n-type PDN (pull-down network) followed by a static inverter, as shown in Figure 33. During precharge, the output of the PDN is charged up to  $V_{DD}$ , and the output of the inverter is set to “0”. During evaluation, the PDN conditionally discharges, and the output of the inverter makes a conditional transition from “0”  $\rightarrow$  “1”. If one assumes that all the inputs of a domino gate are outputs of other domino gates, then it is ensured that all inputs are set to “0” at the end of the precharge phase, and that the only transitions during evaluation are “0”  $\rightarrow$  “1” transitions. The introduction of the static inverter has the additional advantage that the fan-out of the gate is driven by a static inverter with a low-impedance output, which increases noise immunity. Also, the buffer reduces the capacitance of the dynamic output node by separating internal and load capacitances. Finally, the inverter can be used to drive a keeper device to combat charge leakage and charge redistribution.

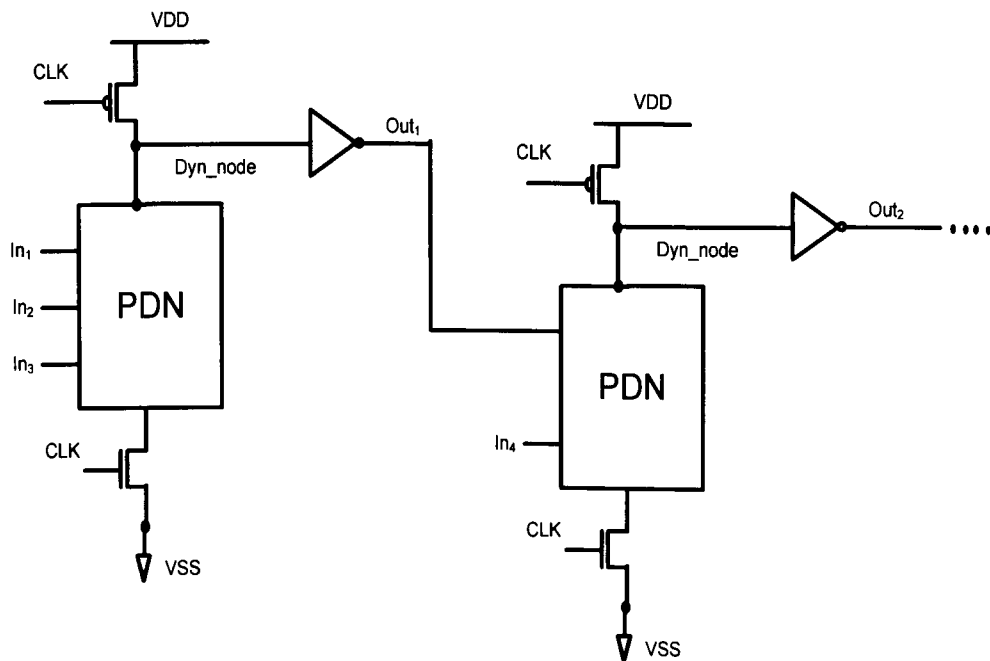


**Figure 33 Domino Logic**

Consider now the operation of a chain of domino gates. During precharge, all inputs are set to “0”. During evaluation, the output of the first domino block either stays at “0” or make a “0” → “1” transition, affecting the second gate. This effect might ripple through the whole chain, one after the other, similar to a line of falling dominoes—hence the name. Domino logic circuit has the following properties:

1. Since each dynamic gate has a static inverter, only non-inverting logic can be implemented.
2. Very high speeds can be achieved: only a rising edge delay exists, while  $T_{pHL}$  (high to low transition time) equals zero. The inverter can be sized to match the fan-out, which is already much smaller than in the complimentary static CMOS case, as only a single gate capacitance has to be accounted for per fan-out gate.

Domino logic clearly can result in high-performance solutions compared to static circuits. However, there are several important considerations that must be taken into account if one wants dynamic circuits to function properly. These include charge leakage and charge sharing.

The operation of a dynamic gate relies on the dynamic storage of the output value on a capacitor. If the pull-down network is *off*, ideally, the output should remain at the precharged state of  $V_{DD}$  during the evaluation phase. However, this charge gradually leaks away due to leakage currents, eventually resulting in a malfunctioning of the gate. Figure 34 shows the sources of leakage for the basic dynamic inverter circuit.

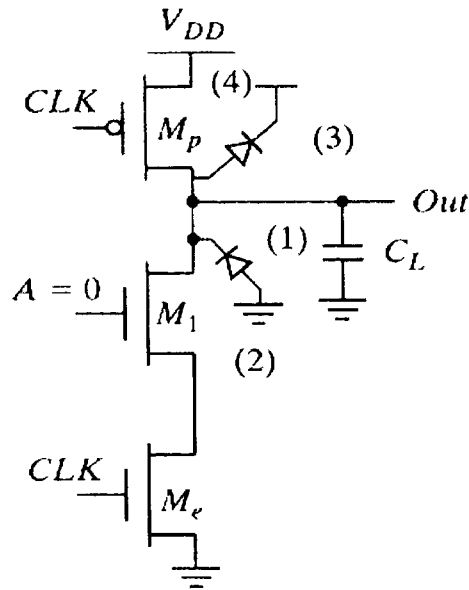


**Figure 34 Leakage issues in dynamic circuits**

Source 1 and 2 are the reverse-biased diode and subthreshold leakage of the NMOS pull-down device  $M_1$ , respectively. The charge stored on  $C_L$  will slowly leak away through these leakage channels, causing degradation in the high level. Dynamic circuits therefore require a minimal clock rate, which is typically on the order of a few KHz. Note that the PMOS precharge device also contributes some leakage current due to the reverse bias diode (source 3) and the subthreshold conduction (source 4). To some extent, the leakage current of the PMOS counteracts the leakage of the pull-down path. As a result, the output voltage is going to be set by the resistive divider composed of the pull-down and pull-up paths.

Leakage is caused by the high-impedance state of the output node during the evaluate mode, when the pull-down path is turned off. The leakage problem may be counteracted by reducing the output impedance on the output node during evaluation. This often is done by adding a keeper transistor. The only function of the keeper-- a PMOS style pull-up device-- is to compensate for the charge lost due to the pull-down leakage paths. To avoid ratio problems associated with this style of circuit and the associated static power

consumption, the keeper resistance is made high (in other words, the device is kept small). This allows the (strong) pull-down devices to lower the Out node substantially below the switching threshold of the next stage. Often, the keeper is implemented in a feedback configuration to eliminate the static power dissipation altogether, as shown in Figure 35.

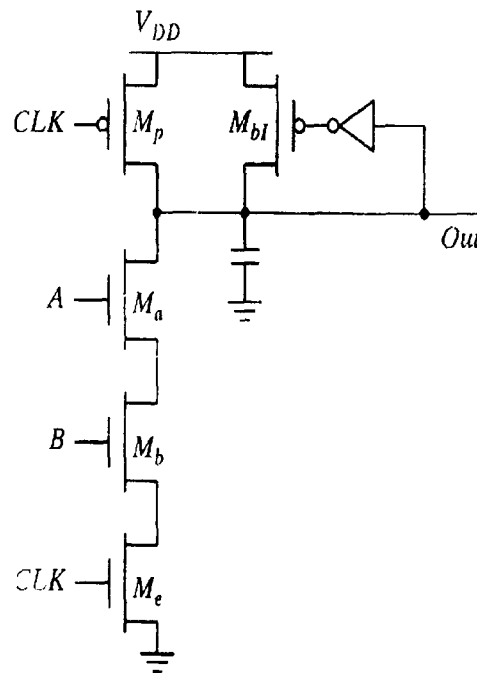


**Figure 35 Static keeper compensate for the charge leakage**

Another important concern in dynamic logic is the impact of charge sharing. Consider the circuit in Figure 36. During the precharge phase, the output node is precharged to  $V_{DD}$ . Assume that all inputs are set to “0” during precharge, and that the capacitance  $C_a$  is discharged. Assume further that input B remains at “0” during evaluation, while input A makes a “0”  $\rightarrow$  “1” transition, turning transistor  $M_a$  on. The charge stored originally on capacitor  $C_L$  is redistributed over  $C_L$  and  $C_a$ . This causes a drop in the output voltage, which cannot be recovered due to the dynamic nature of the circuit.

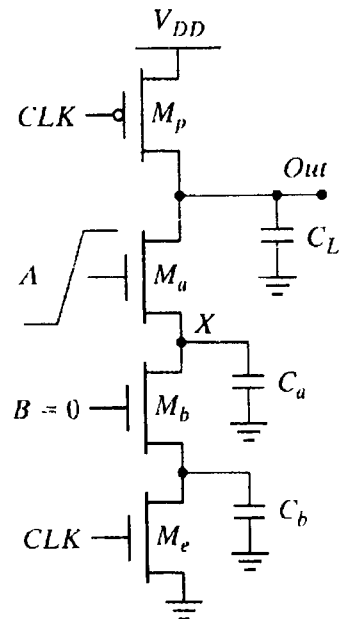


**Figure 36 Charge sharing in dynamic circuits**

The most common and effective approach to deal with the charge redistribution is to also precharge critical nodes. Since the internal nodes are charged to  $V_{DD}$  during precharge, charge sharing does not occur.

The 4:2 compressor is designed in domino logic circuit and shown in Figure 37. It consists of two blocks, each block performs the function of full adder, and these two blocks are cascaded together to realize the function of 4:2 compressor. The first block takes inputs  $A$ ,  $B$  and  $C$ , and generates carry output  $Cout$  and intermediary output  $S$ , the output  $S$  is then passed to the second block with inputs  $D$  and  $Cin$ , generating the output  $Sum$  and  $Carry$ . Within each block, every  $n$ -type PDN is followed by a static inverter and the keeper device (PMOS) is used, as shown in the Figure 37, to compensate for the charge lost due to the pull-down leakage paths.

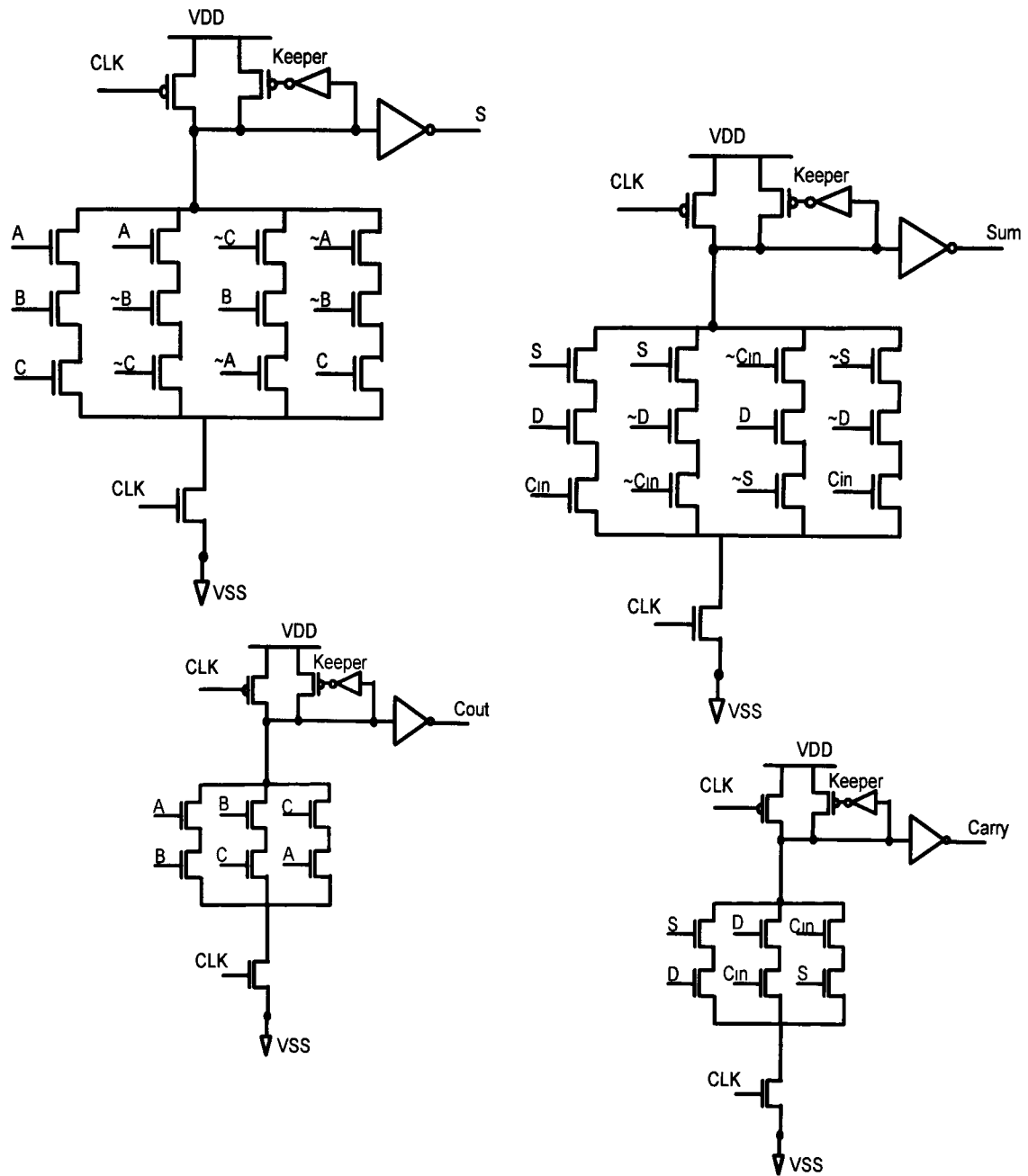


**Figure 37 4:2 compressor in Domino Logic (Com\_D)**

## 4.5 Circuit Level Optimizations of Domino Logic Gates

Several optimizations can be performed on domino logic gates. The most obvious performance optimization involves the sizing of the transistors in the static inverter. With the inclusion of the evaluation devices in domino circuits, all gates precharge in parallel, and the precharge operation takes only two gate delays—charging the output of the dynamic gate to  $V_{DD}$ , and driving the inverter output low. The critical path during evaluation goes through the pull-down path of the dynamic gate and through the PMOS pull-up transistor of the static inverter. Therefore, to speed up the circuit during evaluation, the beta ratio of the static inverter should be made high so that its switching threshold is close to  $V_{DD}$ . This can be accomplished by using a small (minimum-sized) NMOS and a large PMOS device. The minimum-sized NMOS only affects the precharge time, which is generally limited due to the parallel precharging of all gates. The only disadvantage of using a large beta ratio is a reduction in noise margin. Hence, we should consider reduced noise margin and performance impact simultaneously during the transistor sizing.

### 4.5.1 Multiple-output Domino Logic

Numerous variations of domino logic have been proposed. One optimization that reduces area is multiple-output domino logic. The basic concept is illustrated in Figure 38.

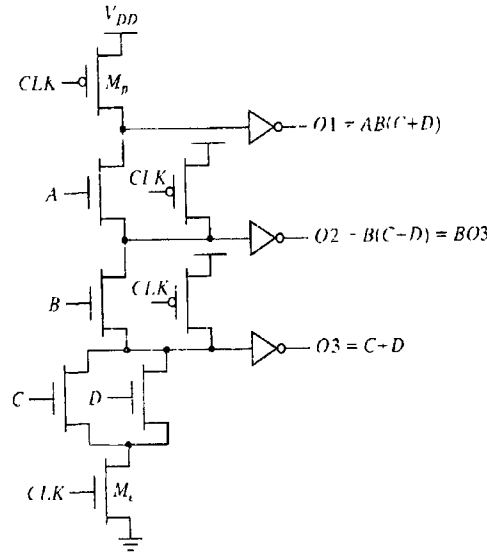


**Figure 38 Multiple-output domino logic**

It exploits the fact that certain outputs are subsets of other outputs to generate a number of logical functions in a single gate. In this example,  $O3 = C + D$  is used in all three outputs, and thus it is implemented at the bottom of the pull-down network. Since  $O2$  equals  $B \cdot O3$ , it can reuse the logic for  $O3$ . Notice that the internal nodes have to be precharged to  $V_{DD}$  to produce the correct results. Given that the internal nodes precharge to  $V_{DD}$ , the number of devices driving precharge devices is not reduced. However, the number of evaluation transistors is drastically reduced because they are amortized over multiple outputs. Additionally, this approach results in a reduction of the fan-out factor, again due to the reuse of transistors over multiple functions [28].

Considering a full adder which takes three equally weighted bits ( $A$ ,  $B$ ,  $C$ ) and produces a sum-bit ( $Sum$ ) as well as a carry-bit ( $Carry$ ), outputs of the full adder can be described as follows:

$$Sum = A \oplus B \oplus C = ABC + \bar{A}\bar{B}C + \bar{A}B\bar{C} + A\bar{B}\bar{C} \quad (1)$$

$$Carry = AB + BC + AC \quad (2)$$



By taking the NOT of *Carry* signal, we obtain:

$$\overline{Carry} = \overline{A} \overline{B} + \overline{B} \overline{C} + \overline{A} \overline{C} \quad (3)$$

Comparing equation (1) with (3), outputs *Sum* and  $\overline{Carry}$  have some parts in common, which are  $\overline{A}B$ ,  $\overline{B}C$  and  $\overline{A}C$ . Therefore, we could use part of the circuit, which is used to generate *Sum* signal, to generate *Carry* signal as well, as shown in Figure 39. Compared with the full adder designed in domino logic (Figure 40), it simplifies the circuit by using one domino gate, instead of two, to realize the functions of full adder.

Furthermore, since 4:2 compressor is formed by two full adders cascaded together, the 4:2 compressor can be realized by using Multiple-output domino logic as shown in Figure 41. The designed circuit consists of two blocks, each block performs the function of full adder, these two blocks are cascaded together to realize the function of a 4:2 compressor. In each full adder block, the output *Carry* is the subset of output *Sum*.

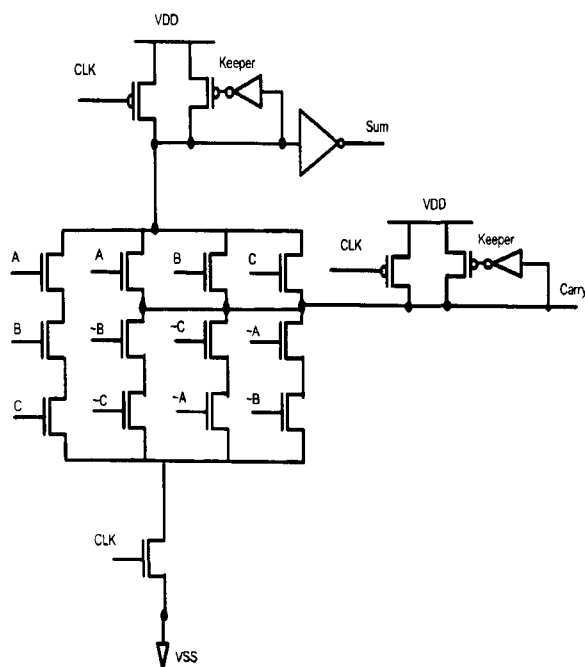


**Figure 39 Full adder in multiple-output domino logic (FA new D)**

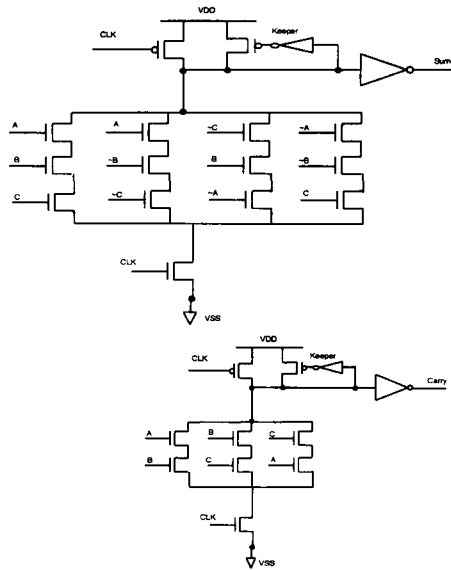


**Figure 40 Full adder in multiple-output domino logic (FA\_D)**

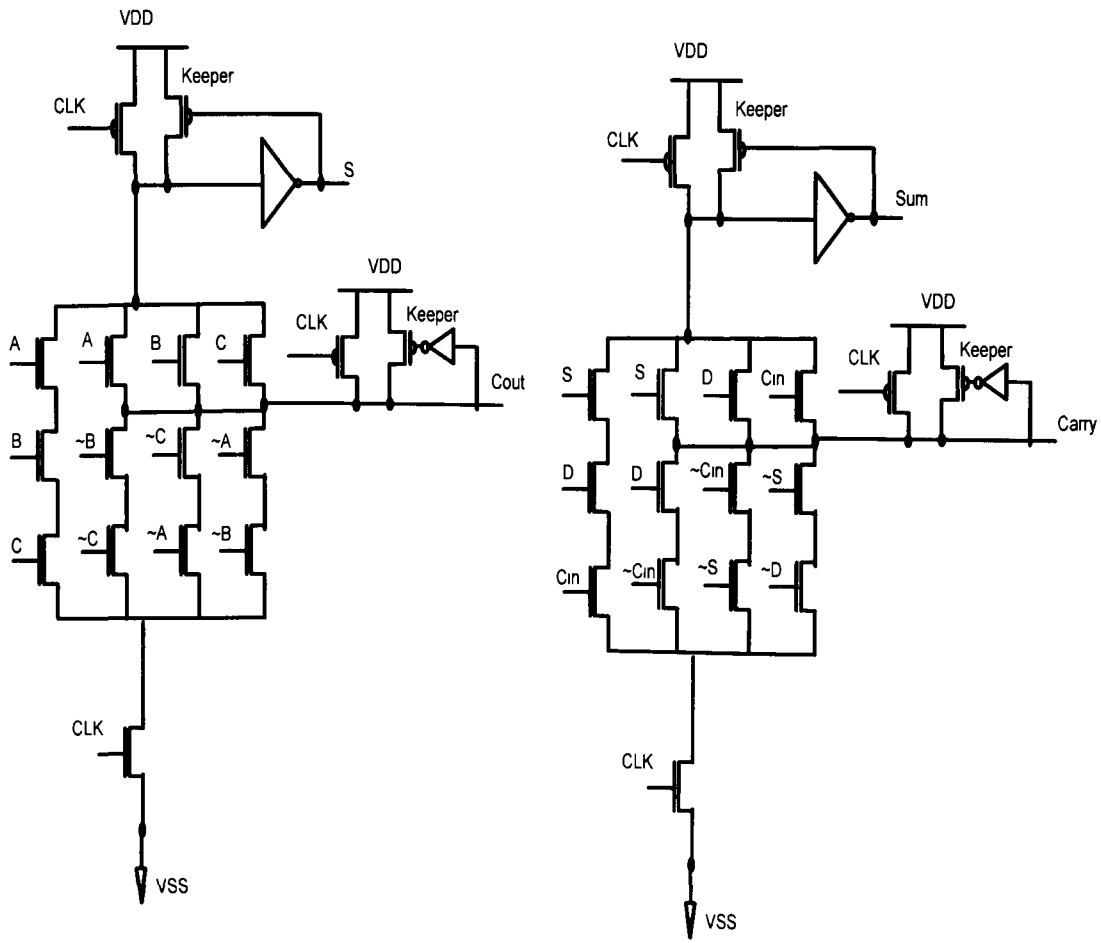


**Figure 414:2 compressor in multiple-output domino logic (Com\_new\_D)**

### 4.5.2 Split Domino Logic

The split domino OR gate shown in Figure 42 achieves higher performance of operation through Splitting the pull-down network into two sub-networks. A logical 2-input NAND operation is then utilized to generate the output. The output inverter is no longer required for the SD circuit. Also, the keeper device is split equally between the two networks.

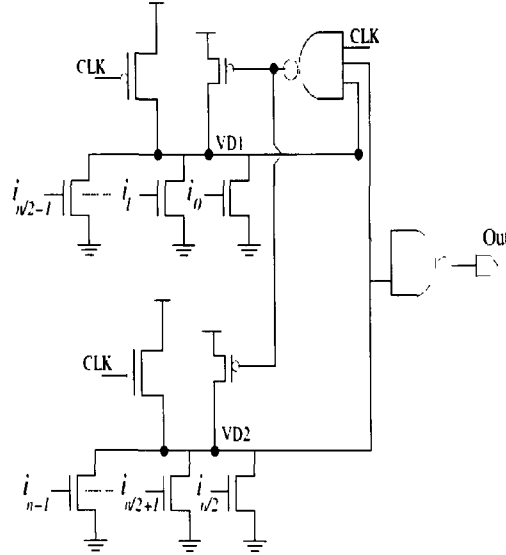


**Figure 42 n-input split domino (SD) OR gate**

Based on the circuit in Figure 39, by splitting the pull-down network into two sub-networks, a full adder is realized in split domino logic, as shown in Figure 43. Moreover, a 4:2 compressor is also designed in split domino logic and shown in Figure 44. It also consists of two blocks, each block performs the function of full adder, these two blocks are cascaded together to realize the function of a 4:2 compressor. The operation of this split domino circuit is described as follows. During precharge, CLK is LOW, the keeper devices are OFF and the output is LOW. At the onset of evaluation, contention is eliminated since keeper devices remain OFF. There are two different cases that need to be considered during the evaluation phase. When all inputs remain LOW and leakage current is at its maximum, the keeper devices controlled by the 3-input NAND gate are quickly activated to prevent the dynamic node from drooping and to keep output noise

within the required limit. The 3-input NAND gate is skewed in such a way to allow for a very fast discharge of the keeper control signal in case all inputs remain LOW. The other case is when the gate evaluates, where at least one path of PDN turns HIGH. In this case, the dynamic node discharges very quickly due to decreased capacitance and nearly keeps the keeper devices in the OFF state and contention is therefore minimized. The main advantage of splitting the pull-down network into two sections is to reduce the dynamic node capacitance and consequently faster evaluation. Also, the large keeper transistor in the conventional case is replaced by another transistor which is nearly half the original keeper size leading to less contention.

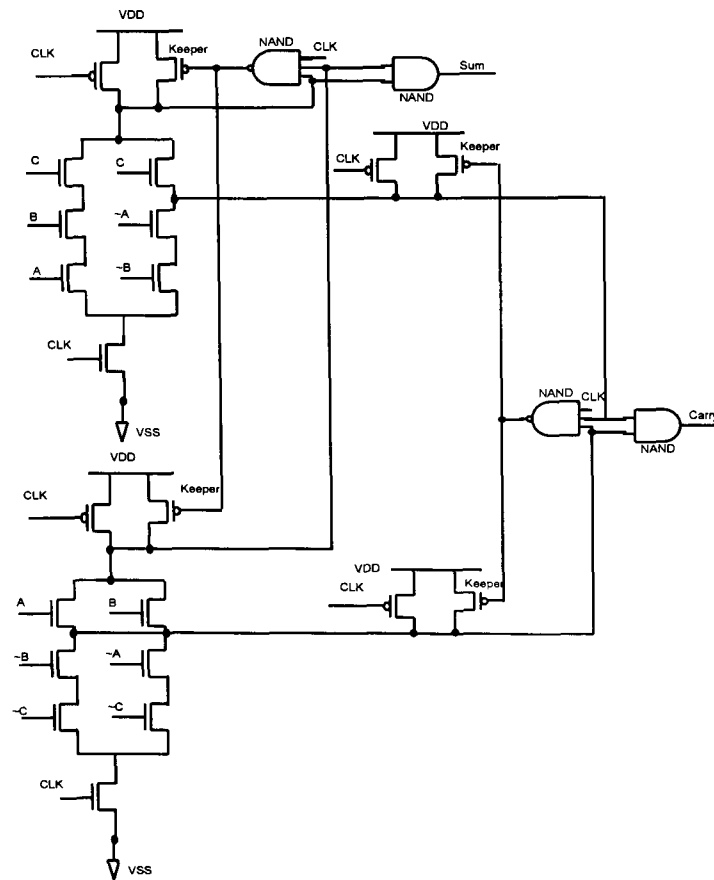


**Figure 43 Full adder in split domino logic (FA\_new\_SD)**

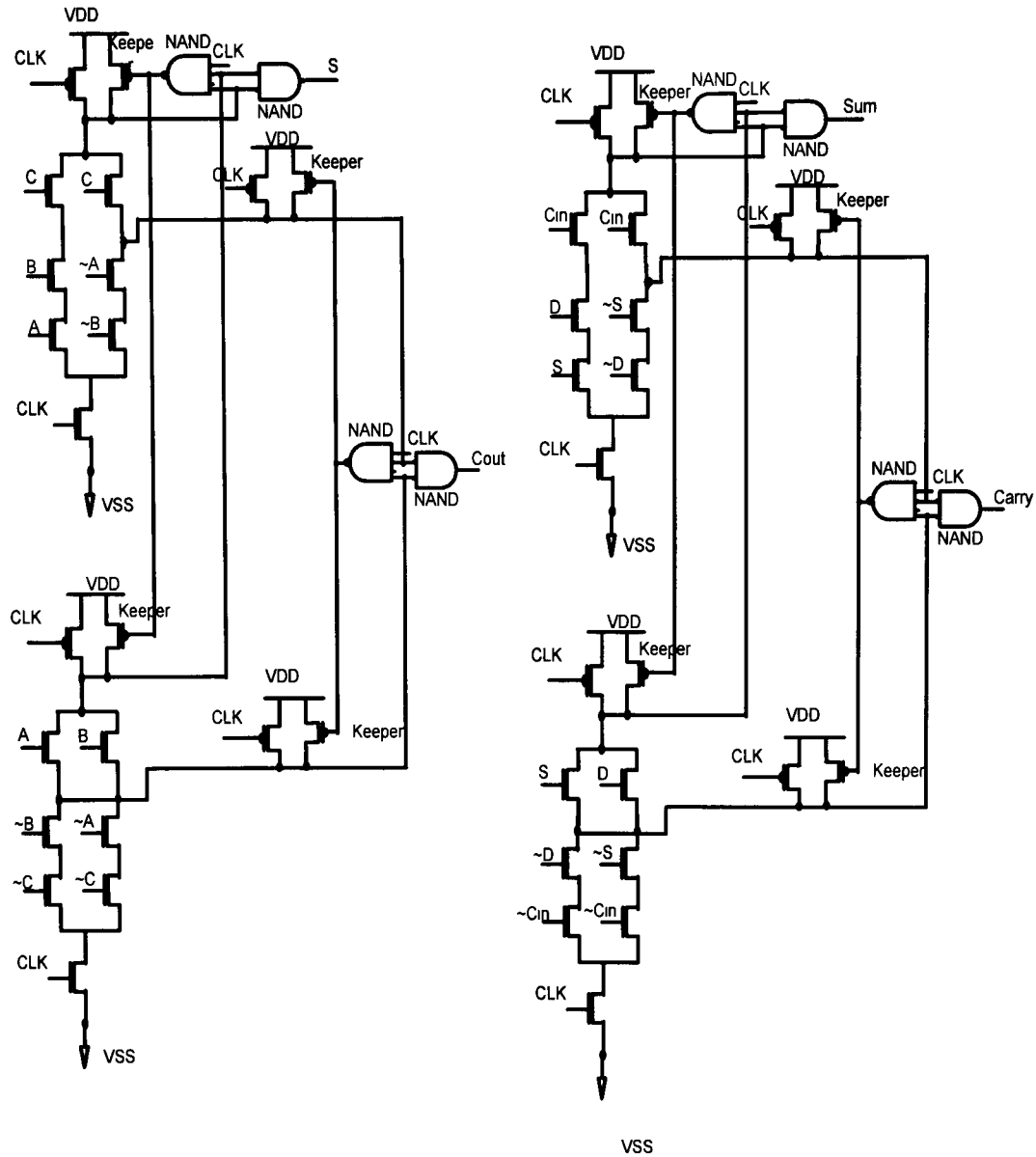


**Figure 44 4:2 compressor in split domino logic (Com\_new\_SD)**

## 4.6 Simulation Result

The simulations are performed by using HSPICE in Cadence design tool. All the circuits are targeted for TSMC 0.18  $\mu\text{m}$  technologies. Therefore, the circuits are designed and optimized based on this process model. All the transistors are sized to achieve the fastest

possible operation frequency as well as the proper functionality. In the test bench, each input is driven by buffered signals and each output is loaded with buffers, which offer a realistic simulation environment reflecting the compressor operation in actual applications. The delay is measured from the time at which the input signals reaching 50% of its full value to the time when the output signal reaching 50% of its full potential. The average delay is the average of delays of all input data. The worst case delay is the largest delay among all input data. Circuits are thoroughly tested by all the possible input vector combinations at 1.8 v voltage source.

#### **4.6.1 Simulation Result for Logical Level Decompositions of 4:2 Compressors**

Three proposed logical level decompositions of 4:2 compressor are simulated. The “Com\_and” in the first row is corresponding to the primitive decomposition of 4:2 compressor in Figure 27. The “Com\_mux” and “Com\_pur\_mux” refer to the two alternative decompositions of 4:2 compressor in Figure 28 (a) and (b) separately. The simulation results and comparison of different implementations are shown in the Table 5 and 6.

**Table 5 Simulation Results for logical decompositions of 4:2 Compressors**

<b>Cell Name</b>	<b>Power Dissipation (ns)</b>	<b>Average Delay (ns)</b>	<b>Worst Case Delay (ns)</b>	<b>Average PDP</b>	<b>Worst Case PDP</b>	<b>Operation Frequency (GHz)</b>
<b>Com_and</b> [Figure 27]	2.48E-04	0.47	0.59	1.17E-13	1.46E-13	1
<b>Com_mux</b> [Figure 28 (a)]	3.12E-04	0.57	0.89	1.78E-13	2.78E-13	0.41
<b>Com_pur_mux</b> [Figure 28 (b)]	2.81E-04	0.51	0.80	1.43E-13	2.25E-13	0.63

**Table 6 Comparison of different logical decompositions of 4:2 Compressors**

<b>Cell Name</b>	<b>Power Dissipation (ns)</b>	<b>Average Delay (ns)</b>	<b>Worst Case Delay (ns)</b>	<b>Average PDP</b>	<b>Worst Case PDP</b>	<b>Operation Frequency (GHz)</b>
<b>Com_and</b> [Figure 27]	100%	100%	100%	100%	100%	100%
<b>Com_mux</b> [Figure 28 (a)]	126%	121%	151%	154%	190%	41%
<b>Com_pur_mux</b> [Figure 28 (b)]	113%	109%	136%	122%	154%	63%

\* All values of “Com\_and” are taken as “1”

As shown in tables, all three decompositions are simulated in terms of delay and power consumption. Power delay product (PDP) is also considered since it is a good metric for gauging performance of the circuitry [8]. The operation frequency is maximum working frequency for each circuit, beyond which the circuit fails to function correctly.

Simulation result indicates that the primitive decomposition of 4:2 compressor (Com\_and) has the best performance. Compared with alternative decompositions of 4:2 compressor (Com\_mux and Com\_pur\_mux), it reduces the average delay and worst case delay by 21%, 9% and 51%, 36% separately, and it saves the power consumption by 26% and 13% respectively. Moreover, its operation frequency is about 2.44 and 1.59 times of that of two alternative decompositions separately. The main reason of compressor Com\_mux and Com\_pur\_mux have higher power consumption and longer delay time compared with compressor Com\_and is that, a large number of static inverters are used to generate complementary input signals for multiplexors.

#### **4.6.2 Simulation Result for Circuit Level Implementations of Full adders and 4:2 Compressors**

Three circuit level design of full adder are simulated. The first full adder is designed in domino logic in Figure 40, which is denoted as “FA\_D” The second full adder is designed in multiple-output domino logic in Figure 39, which is denoted as “FA\_new\_D” The last circuit implements is the full adder in split domino logic in Figure 43, it is denoted as “FA\_new\_SD” The simulation result and comparison of different implementations are shown in Table 7 and 8. All the full adder circuits are simulated in terms of delay and power consumption. The operation frequency is maximum working frequency for each circuit, beyond which the circuit fails to function correctly.



**Table 7 Simulation Result for full adders**

<b>Cell Name</b>	<b>Power Dissipation (ns)</b>	<b>Average Delay (ns)</b>	<b>Worst Case Delay (ns)</b>	<b>Average PDP</b>	<b>Worst Case PDP</b>	<b>Operation Frequency (GHz)</b>
<b>FA_D</b> [Figure 40]	1.78E-04	0.28	0.41	4.98E-14	7.29E-14	1.92
<b>FA_new_D</b> [Figure 39]	1.20E-04	0.29	0.51	3.48E-14	6.12E-14	1.67
<b>FA_new_SD</b> [Figure 43]	1.32E-04	0.22	0.39	2.90E-14	5.15E-14	2.17

**Table 8 Comparison of Simulation Result**

<b>Cell Name</b>	<b>Power Dissipation (ns)</b>	<b>Average Delay (ns)</b>	<b>Worst Case Delay (ns)</b>	<b>Average PDP</b>	<b>Worst Case PDP</b>	<b>Operation Frequency (GHz)</b>
<b>FA_D</b> [Figure 40]	100%	100%	100%	100%	100%	100%
<b>FA_new</b> [Figure 39]	67%	104%	124%	70%	84%	87%
<b>FA_new_SD</b> [Figure 43]	74%	79%	95%	58%	71%	113%

\* All values of “FA\_D” are taken as “1”

According to the simulation result, in terms of power consumption, full adder in multiple-output domino logic has the best performance, since it has the lowest transistor count, it reduces the power consumption by 33% compared to the full adder in domino logic. Because of low dynamic node capacitance, the full adder in split domino logic reduces delay by 21% and increase operation frequency by 13% compared to the full adder in domino logic.

Three circuit level design of 4:2 compressor are simulated. The first circuit is the design of 4:2 compressor in domino logic in Figure 37, which is denoted as “Com\_D” The second one is the design of 4:2 compressor in multiple-output domino logic in Figure 41, which is denoted as “Com\_new\_D” The last circuit implements the 4:2 compressor in split domino logic in Figure 44, it is denoted as “Com\_new\_SD” The simulation result and comparison of different implementations are shown in Table 9 and 10. All the compressor circuits are simulated in terms of delay and power consumption. The operation frequency is maximum working frequency for each circuit, beyond which the circuit fails to function correctly.

***Table 9 Simulation Result for 4:2 compressors***

<b>Cell Name</b>	<b>Power Dissipation (ns)</b>	<b>Average Delay (ns)</b>	<b>Worst Case Delay (ns)</b>	<b>Average PDP</b>	<b>Worst Case PDP</b>	<b>Operation Frequency (GHz)</b>
<b>Com_D</b> <b>[Figure 37]</b>	2.48E-04	0.47	0.60	1.17E-13	1.49E-13	1
<b>Com_new_D</b> <b>[Figure 41]</b>	2.29E-04	0.42	0.53	0.96E-13	1.21E-13	1.25
<b>Com_new_SD</b> <b>[Figure 44]</b>	2.27E-04	0.32	0.48	0.73E-13	1.09E-13	1.67

**Table 10 Comparison of Simulation Result**

<b>Cell Name</b>	<b>Power Dissipation (ns)</b>	<b>Average Delay (ns)</b>	<b>Worst Case Delay (ns)</b>	<b>Average PDP</b>	<b>Worst Case PDP</b>	<b>Operation Frequency (GHz)</b>
<b>Com_D</b> [Figure 37]	100%	100%	100%	100%	100%	100%
<b>Com_new</b> [Figure 41]	92%	89%	88%	82%	81%	125%
<b>Com_new_SD</b> [Figure 44]	91%	68%	80%	62%	73%	167%

\* All values of “Com\_D” are taken as “1”

Simulation result indicates that 4:2 compressor designed in split domino logic (Com\_new\_SD) has the best performance. Compared with the first circuit (Com\_D), it reduces the average delay and worst case delay by 32% and 20%. Since it has lower transistor count, it saves the power consumption by 9%. Consequently, it achieves 38% and 27% savings in terms of average PDP and worst case PDP. Moreover, due to its reduced dynamic node capacitance, the operation frequency of “Com\_new\_SD” is about 1.67 times of that of “Com\_D”

According to Table 10, the 4:2 compressor circuit in multiple-output domino logic (Com\_new\_D) outperform the first circuit (Com\_D) in terms of delay and operation frequency. However, in Table 8, the full adder circuit in multiple-output domino logic (FA\_new\_D), which is the building block of 4:2 compressor in multiple-output domino logic, has longer delay and lower operation frequency than that of the first circuit (FA\_D),

which is the building block of circuit (Com\_D). The reason is that: when we design the full adder in multiple-output domino logic, the total dynamic node capacitance is increased, thus increase the delay and reduce the operation frequency. However, when we cascade the full adder in multiple-output domino logic to realize the 4:2 compressor, in order to make the circuit work properly, we have to increase the fan-out of full adder block, thus transistor sizing is applied to each pull-down network. This reduces the total dynamic node capacitance of the circuit, and consequently reduces the delay and increase the operation frequency of the circuit.

# **CHAPTER 5**

## **CONCLUSIONS**

### **5.1 Summary of Contributions**

The purpose of this study has been to explore digital multiplication at both architectural level and transistor level. This leads to several contributions in the digital multiplication architecture and high speed low power digital circuit design.

#### **5.1.1 Architectural Contributions**

The recursive multiplier architecture has been further explored with the utilization of an optimized 4:2 compressor reduction scheme which is smaller and more logically efficient than those proposed in the past. The single level recursive multiplier has then been enhanced with some gating multiplexors and a majority voter forming a novel reconfigurable multiplier architecture. This proposal has been implemented and simulated on the 0.18  $\mu\text{m}$  CMOS process. Its performance and overall characteristics have been compared against a standard Booth-recoded Wallace multiplier of the same size.

### **5.1.2 Transistor Level Contributions**

Based on the primitive logical decomposition of 4:2 compressor, three different circuitries of 4:2 compressor in Domino logic are proposed, simulation results have provided validation for these designs.

## **5.2 Conclusions**

By targeting many of the contemporary requirements for digital systems such as power consumption, critical path delay, regularity, and fault tolerance, a reconfigurable multiplier architecture that embodies these characteristics has been developed. This architecture utilizes the recursive multiplication algorithm and an optimized 4:2 compressor layout scheme for partial product reduction.

The developed reconfigurable multiplier architecture has been implemented using the TSMC 0.18  $\mu\text{m}$  CMOS standard cell libraries and its performance has been compared against a typical multiplier architecture, namely a Booth-recoded Wallace Tree multiplier. The simulation results have demonstrated that, on average, the reconfigurable multiplier is efficient in terms of power consumption. The new scheme offers over a 25% savings in cell internal power and a 19% decrease in dynamic power consumption respectively. In addition, this scheme has a slightly shorter delay time, which benefits from the regularity of recursive structure.

To further enhance the performance of proposed reconfigurable multiplier, three circuit level implementations of 4:2 compressor, which is widely used in highly efficient partial product reduction, have been proposed and simulated by using HSPICE. The simulation result confirms that the 4:2 compressor designed in split domino logic has the best performance among all three designs. Due to its reduced dynamic node capacitance, it increases its operation frequency by 67% and reduces the average delay by 32%, as compared to the bench mark 4:2 compressor which is designed in domino logic.

# REFERENCES

- [1] Gary. W Bewick, "Fast Multiplication: Algorithms and Implementation", Dissertation for the Degree of Doctor in Philosophy, Stanford University, 1994.
- [2] Bickerstaff, Schulte and E.E. Swartzlander Jr., "Analysis of column compression multipliers", IEEE Symposium on Computer Arithmetic, pp. 33 -39, 2001.
- [3] Behrooz Parhami, "Computer Arithmetic: Algorithms and Hardware Designs", Oxford University Press, New York, 2000.
- [4] C.S. Wallace, "A suggestion for a fast multiplier", IEEE Transactions on Electronic Computers, vol. 13, pp 14-17, 1964.
- [5] Luigi Dadda, "Some schemes for parallel multipliers", Alta Frequenza, vol. 45, pp. 574-580, 1966.
- [6] A. Karatsuba and Y. Ofman, "Multiplication of Multidigit Numbers on Automata", Sov. Phys.-Dokl. (English Translation), vol. 7, pp. 595-596, 1963
- [7] A. Habibi and P.A. Wintz, "Fast Multipliers", IEEE Transactions on Computers, vol. C-19, pp. 153-157, 1970.
- [8] W Stenzel, W. Kubitz, G. Garcia, "A Compact High-Speed Parallel Multiplication. Scheme", IEEE Transactions on Computers, vol. 26, pp. 948-957, 1977.
- [9] A. Weinberger, "4:2 Carry-Save Adder Module", IBM Technical Disclosure Bulletin, vol. 23, Jan. 1981.
- [10] P.Mokrian, "A reconfigurable digital multiplier architecture," Master thesis, University of Windsor, 2003.
- [11] G. Michael Howard , "Investigation into arithmetic sub-cells for digital multiplication," Master thesis, University of Windsor, 2005.
- [12] A.N. Danysh, and E.E. Swartzlander Jr., "A recursive fast multiplier", Asilomar Conference on Signals, Systems & Computers, vol. 1, pp. 197 -201, 1998.
- [13] C. Paar, "A new architecture for a parallel finite field multiplier with low complexity based on composite fields". IEEE Transactions on Computers, vol. 45, pp. 856-861, 1996.

- [14] Peter Cameron, "Encyclopaedia of Design Theory", <http://www.maths.qmul.ac.uk/~pjc/design/encyc/topics/>, 2002.
- [15] J. Kim and E.E. Swartzlander Jr., "Improving the recursive multiplier", Asilomar Conference on Signals, Systems and Computers, vol. 2, pp. 1320 -1324, 2000.
- [16] R. Rogenmoser, L. O'Donnell, S. Nishimoto, "A dual-issue floating-point coprocessor with SIMD architecture and fast 3D functions", IEEE International Solid-State Circuits Conference, Volume: 1m pp. 414 -415, 2002.
- [17] R.K. Kolagotla, J. Fridman, B.C. Aldrich, M.M. Hoffman, W.C. Anderson, M.S. Allen, D.B. Witt, R.R. Dunton, L.A.Booth Jr., "High performance dual-MAC DSP architecture", IEEE Signal Processing Magazine , Volume: 19 Issue: 4 , pp. 42 -53, July 2002.
- [18] J. Eyre and J. Bier, "The evolution of DSP processors", IEEE Signal Processing Magazine, vol. 17 Issue: 2 , pp. 43-51, March 2000.
- [19] Reto Zimmermann, "Computer Arithmetic: Principles, Architectures, and VLSI Design", Lecture notes for the Integrated Systems Laboratory, Swiss Federal Institute of Technology (ETH), 1999.
- [20] R. Kaivola, N. Narasimhan, "Formal Verification of the Pentium 4 Floating-Point Multiplier", Design, Automation and Test in Europe Conference and Exhibition, pp. 20-27, 2002.
- [21] A. D. Booth, "A Signed Binary Multiplication Technique", Quarterly Journal of Mechanics and Applied Mathematics, vol. 4, pp 236–240, June 1951.
- [22] P.J. Song, G. De Micheli, "Circuit and architecture trade-offs for high-speed multiplication" IEEE Journal of Solid-State Circuits, vol 26, pp. 1184-1198, 1991.
- [23] M. Mehta, V Parmar, E. Swartzlander, "High-speed multiplier design using multiinput counter and compressor circuits", IEEE Symposium on Computer Arithmetic, pp. 43-50, 1991.
- [24] R.V.K. Pillai, D. Al-Khalili and A.J. Al-Khalili, "Energy delay analysis of partial product reduction methods for parallel multiplier implementation", International Symposium on Low Power Electronics and Design, pp. 201 -204, 1996.



- [25] D. Villeger and V.G. Oklobdzija, "Analysis of Booth encoding efficiency in parallel multipliers using compressors for reduction of partial products", Asilomar Conference on Signals, Systems and Computers, vol. 1, pp. 781 -784, 1993
- [26] Pascal Bonatto and Vojin Oklobdzija, "Evaluation of Booth's algorithm for implementation in parallel multipliers", Asilomar Conference on Signals, Systems and Computers, vol. 1, pp. 608 -610, 1996.
- [27] Chip-Hong Chang, Jiangmin Gu, and Mingyan Zhang, "Ultra low-voltage low-power CMOS 4-2 and 5-2 compressors for fast arithmetic circuits," IEEE Transactions on Circuits and Systems, vol. 51, no.10, Oct. 2004.
- [28] Jan M. Rabaey, "Digital integrated circuits- a design perspective," Prentice-Hall, New Jersey, 2003.
- [29] Zimmermann and Fichtner, "Low-Power Logic Styles: Cmos Versus Pass-Transistor Logic", IEEE Journal of Solid-State Circuits, vol. 32, pp.1079-1090, July 1997.
- [30] Massoud Pedram, "Power Optimization and Management in Embedded Systems", Asia and South Pacific Design Automation Conference, pp. 239 -244, 2001G. Binnig, C. F Quate, and C. Gerber, "Atomic Force Microscope," Phys. Rev. Lett., vol. 56, pp. 930-933, Mar. 1986.

# VITA AUCTORIS

Peng Chang was born in 5 Nov, 1981 in Nan Yang, He Nan, China. He obtained his B.A.Sc. in Electrical and Computer Engineering from Central South Forestry University in Hu Nan, China, where he graduated in 2005.

In Fall 2006, Peng began the pursuit of a M.A.Sc. degree in Electrical Engineering under the supervision of Dr. Majid Ahmadi at the University of Windsor, Windsor, Ontario, Canada. During this period, he has received a University of Windsor Tuition Scholarship. His area of specialization has been the high speed low power digital multiplier design.